Nanoscale

RSC Publishing

REVIEW

View Article Online
View Journal | View Issue

Nano–bio effects: interaction of nanomaterials with cells

Cite this: *Nanoscale*, 2013, **5**, 3547

Liang-Chien Cheng,†[a] Xiumei Jiang,†[b] Jing Wang,[b] Chunying Chen*[b] and Ru-Shi Liu*[ac]

With the advancements in nanotechnology, studies on the synthesis, modification, application, and toxicology evaluation of nanomaterials are gaining increased attention. In particular, the applications of nanomaterials in biological systems are attracting considerable interest because of their unique, tunable, and versatile physicochemical properties. Artificially engineered nanomaterials can be well controlled for appropriate usage, and the tuned physicochemical properties directly influence the interactions between nanomaterials and cells. This review summarizes recently synthesized major nanomaterials that have potential biomedical applications. Focus is given on the interactions, including cellular uptake, intracellular trafficking, and toxic response, while changing the physicochemical properties of versatile materials. The importance of physicochemical properties such as the size, shape, and surface modifications of the nanomaterials in their biological effects is also highlighted in detail. The challenges of recent studies and future prospects are presented as well. This review benefits relatively new researchers in this area and gives them a systematic overview of nano–bio interaction, hopefully for further experimental design.

Received 25th December 2012
Accepted 7th March 2013

DOI: 10.1039/c3nr34276j

www.rsc.org/nanoscale

1 Introduction

Nanotechnology has become a research hotspot because of its extremely small size that enables potential use in wide-ranging applications.[1] Nanomaterials (NMs) are a combination of a group of atoms and molecules possessing advantageous chemical and physical properties that significantly vary from their bulk counterparts. NMs are the transition state between bulk materials and molecular clusters. Thus, NMs remarkably diverge from traditional macro- or micro-perspectives, showing unique optical, magnetic, electrical, chemical, and mechanical properties.[1–3]

Recently, NMs have been widely investigated because of their potential applications in biomedicine, surface enhanced Raman spectroscopy, and catalysis. The outstanding properties of NMs make them appropriate for utilization in various biological and medical systems, including cancer and gene

[a]*Department of Chemistry, National Taiwan University, Taipei 106, Taiwan. E-mail: rsliu@ntu.edu.tw; Fax: +886-2-33668671; Tel: +886-2-33661169*

[b]*CAS Key Laboratory for Biomedical Effects of Nanomaterials and Nanosafety, National Center for Nanoscience and Technology, Beijing 100190, China. E-mail: chenchy@nanoctr.cn; Fax: +86-10-62656765; Tel: +86-10-82545560*

[c]*Genomics Research Center, Academia Sinica, Taipei 115, Taiwan*

† These authors contributed equally to this work.

Liang-Chien Cheng is currently a PhD student at the Department of Chemistry, National Taiwan University, supervised by Prof. Ru-Shi Liu. He received his MS degree in Chemistry from National Sun Yat-sen University in 2008. His current research interests include the synthesis of metallic NPs, nanodiamonds and the upconversion NMs for bio-applications.

Xiumei Jiang is a PhD student at the CAS Key Laboratory for Biomedical Effects of NMs and Nanosafety, National Center for Nanoscience and Technology of China. She received her Bachelor's Degree in Biology from Northeast Normal University, China (2010). Her research interests include the biomedical application and potential toxicity of NPs in cancer therapy.

therapies, photothermal and photodynamic therapy, bioimaging, diagnostics, bioanalytical methods, and pharmacokinetics studies.[1,4–6] Thus, interactions between NMs and cells present the most primitive fundamental phenomenon, and highlight the importance of basic research. Most bio-applications, including drug delivery, bioimaging, or therapeutic treatments, begin from the attachment of NMs onto targeting cells. The versatile behaviors are highly dependent on the physical and chemical properties of NMs. In this review, we discuss the influences of the morphology, size, surface charge, surface modifications, and chemical compositions of NMs on cells based on recent studies. We also summarize the cellular uptake, intracellular trafficking, and cytotoxicity of different kinds of NMs. Strategies on how to improve the interactions between NMs and cells, as well as their future applications in biological systems are discussed in detail.

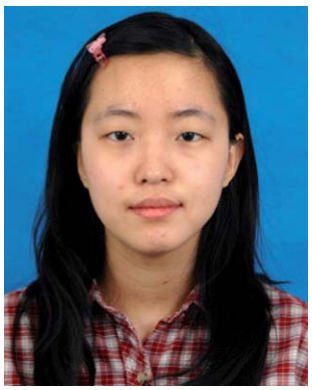

Jing Wang is a masters student at the CAS Key Laboratory for Biomedical Effects of NMs and Nanosafety, National Center for Nanoscience and Technology of China. She obtained her Bachelor's Degree in Chemistry at the China Agricultural University in 2011. Her research field mainly involves NPs as a multifunctional theranostic platform for cancer therapy.

Chunying Chen is a principal investigator at the CAS Key Laboratory for Biomedical Effects of NMs and Nanosafety, National Center for Nanoscience and Technology of China. Dr Chen received her Bachelor's Degree in Chemistry (1991) and obtained her PhD in Biomedical Engineering (1996) from Huazhong University of Science and Technology of China. Her research interests include the potential toxicity of NPs, therapies for malignant tumors using theranostic nanomedicine systems that carry chemotherapeutics and imaging tags, and vaccine nanoadjuvants using NMs as a potential nonviral adjuvant. Her research is supported by the China MOST 973 Program, Natural Science Foundation of China, EU-FP6 and FP7, and IAEA. She has authored/co-authored over 100 peer-reviewed papers, two books, and ten book chapters. She is an Editorial Board Member at Current Drug Metabolism.

2 Nanostructured materials and their fabrication

NMs are of great scientific interest because their properties are a bridge between their molecular and bulk species. Their remarkable changes in the nanoscale can be divided into three main physical effects.

I Surface effect

Compared with bulk materials, nanoparticles (NPs) have a small size that ensures a high percentage of surface atoms at or near interfaces and a high surface energy. The specific surface area is defined as the ratio of the surface area to volume.[7] With decreased particle size, the surface atoms greatly increase and the atomic coordination numbers decrease. Consequently, the surface energy is high, leading to high reactivity of these surface atoms and ease in combining with the other atoms. In catalysis, the surface energy is directly proportional to the size effect. To increase catalysis and reactivity, the NP size must be decreased.

II Small scale effect

With decreased particle size to the nanoscale or even smaller, the regular boundary condition of crystals becomes destructive, and the surface molecular density of amorphous NPs decreases. This phenomenon changes their physical properties, such as optical, thermal, magnetic, and mechanical. The small scale effect is defined as macroscopic changes in their physical properties with decreased particle size. The main properties are presented as follows.

(1) Optical property. The optical property of nanostructured materials is correlated with their internal structure, such as the electronic state, defect, and band structure. The small particles,

Ru-Shi Liu is currently a professor at the Department of Chemistry, National Taiwan University. He received his Bachelor's Degree in Chemistry from Shoochow University (Taiwan) in 1981. He received his Master's Degree in Nuclear Science from the National TsingHua University (Taiwan) in 1983. He obtained two PhDs in Chemistry: one from National TsingHua University in 1990 and another from the University of Cambridge in 1992. He worked at Materials Research Laboratories at the Industrial Technology Research Institute from 1983 to 1985. He was an associate professor at the Department of Chemistry of National Taiwan University from 1995 to 1999, and was promoted to professorship in 1999. His research concerns the field of Materials Chemistry. He is an author or coauthor of more than 400 studies published in scientific international journals. He has also been granted more than 80 patents.

large surface area, and irregular conformation of atomic arrangement lead to a novel optical property different from their bulk states. With decreased NP size, the surface tension increases and the bond length decreases, leading to enhanced vibrational frequency and a blue shift in the optical property. According to the quantum size effect, the band gap increases and influences the absorption of materials at long wavelengths. As the particle size decreases near or below the Bohr radius of the semiconductors, the band gap increases, and then the absorption and fluorescence spectra blue shift. In other words, the particle size directly influences the optical property. By contrast, in the case of noble metal NPs, the metal particles are black and the particle size is smaller than the irradiative wavelength. The color becomes darker with decreased size. However, the free electrons of noble metal NPs are excited by incident light and undergo a collective coherent oscillation known as localized surface plasmon resonance. In other words, noble metal NPs show strong absorption bands in the ultraviolet, visible, or infrared regions because of their localized surface plasmon oscillation.[8,9]

(2) Thermal dynamic property. Solid materials in their bulk state have a fixed melting point. As the size decreases to <10 nm, the melting point markedly increases because of the change in chemical potential energy. With further decreased particle size down to nanometers, the specific surface area and, in turn, the thermal dynamic property is altered.[10]

(3) Magnetic property. With decreased size from bulk materials, the magnetic phenomenon becomes directly independent of size changes. The magnetic structures of bulk materials are made of several magnetic domains; however, a single nanocrystal owns a single magnetic domain. In other words, with decreased size, the magnetic domain of strong magnetic particles is transferred from a multi-magnetic domain into a single magnetic domain, which leads to the orientation of electron spins becoming antiparallel to the super-exchange interaction. The coercive force of magnetite is also size dependent. The magnetic domain transforms from paramagnetic to super-paramagnetic with decreased size because of the simultaneous decrease in coercive force.[11]

(4) Mechanical property. The mechanical property of small-sized particles shows high toughness and malleability because their complicated molecular arrangement can be easily altered through force compression. The lack of NM coordination and strong van der Waals force confer the nanocomposites with excellent mechanical properties.

III Quantum size effect

As aforementioned, the size effect is important because the electron band gap of the Fermi level changes from continuous to discrete with decreased size. Semi-conductor NPs with sizes below the Bohr radius lead to an increase in the band gap energy, and cause the highest occupied molecular orbital and lowest unoccupied molecular orbital to break into quantized energy levels. The particle sizes of quantum dots (QDs) directly influence their emission through the quantum confinement effect.[12]

As previously discussed, the small size effect, surface effect, and quantum effect directly influence the physical and chemical properties of nanostructured materials. This phenomenon is verified from their bulk formations and widely observed in several materials. For example, conductive bulk metals become non-conductive metals with decreased size; ferromagnetic substances change their multiple magnetic domain into a single magnetic domain in the nanoscale; and the inert metal platinum can become highly reactive catalyst NPs.[13] Considering the specific interaction and novel effects of these NMs that are between bulk and molecular materials, the science of NMs becomes a new focus of materials science research. Most of these materials have different characteristics with decreased sizes down to nanometers. The next section discusses metal-based, carbon-based, and semiconductor NMs.

2.1 Noble metal-based NMs

Colloidal gold (Au) was first produced by Michael Faraday, who found that fine particles are produced by the reduction of Au chloride and stabilization of carbon disulfide. Nowadays, colloidal NP syntheses mostly take a similar route, *i.e.*, the reduction of Au salt precursors and subsequent surface protection by stabilizers. To generate different morphologies or sizes for tuning chemical or physical properties, the synthesis routes have evolved into versatile methods.[5]

The most commonly used method for fabricating NPs is the citrate method. Turkevich *et al.* first applied a citrate method that uses citrate as a reduction agent and stabilizer, and Au NPs ranging from 9 nm to 120 nm in size are obtained.[14] Lee and Meisel used a citrate method to synthesize colloidal silver (Ag) NPs.[15] The procedures of both citrate methods are the same. The metal precursors are reduced by citrate in a boiling aqueous solution and then stabilized by citrate. However, this simple synthesis process tends to yield NPs with random morphologies. To control these morphologies, the method is modified under specific conditions. Such morphology control approaches are widely discussed. The concentration of metal precursors directly influences the NP sizes. The pH of the reaction solution influences the protonation states of citrate ion and changes the reduction rate, thereby yielding NPs with different sizes and morphologies. The synthesis temperature also affects the NP shapes. The citrate method has evolved into mixing external metal precursors for morphology sculpture. This method is attracting increased attention because citrate can be easily substituted by other biological thiol terminal ligands.[16] Thiol terminal proteins, DNA, and siRNA capping agents can easily replace citrate because of the strong conjugation between Au and sulfur. For further bio-applications, the replacement of the citrate ligand with a bio-friendly, targeting, or fluorescent ligand can lead to increased applications in biological systems.

In addition, the seed-growth method is gaining considerable interest because of its remarkable size and morphology-controlled process.[17] As the technique name suggests, metal salts are reduced by a strong reducing agent to fabricate small, spherical, seed-mediated particles in an aqueous solution. The nucleation and growth processes are separated for better morphology control. NP surfaces are surrounded by surfactants that are used to stabilize the materials during the reactions. To

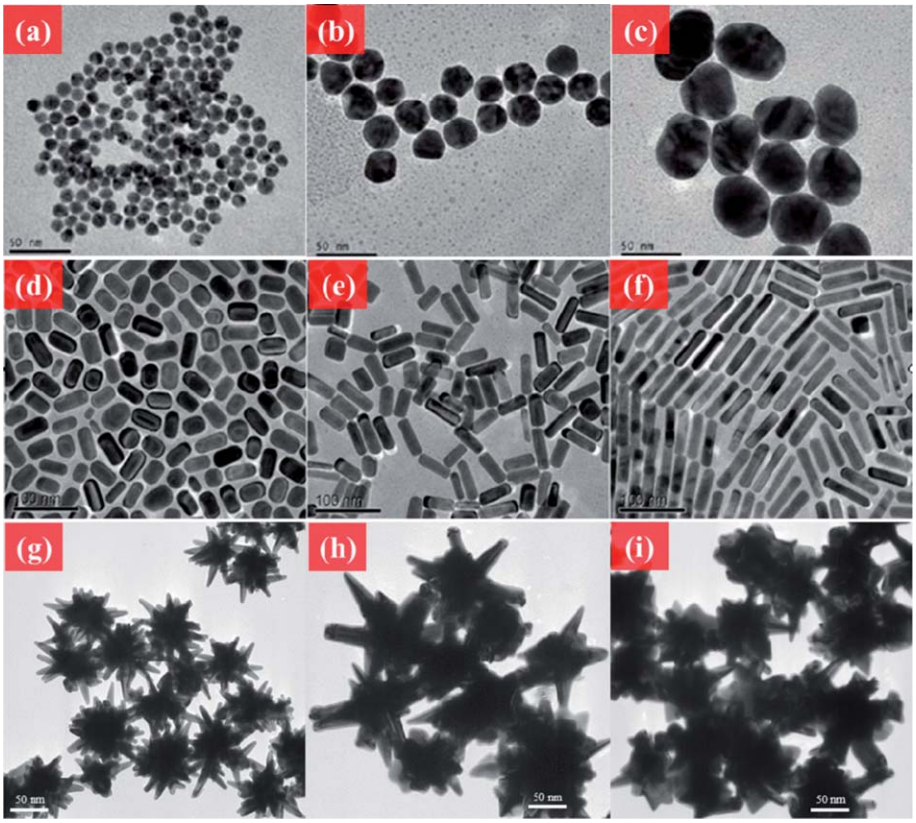

Fig. 1 TEM images of Au NMs. (a–c) Au NPs in different sizes. (d–f) CTAB-coated Au NRs with different aspect ratios. (g–i) Au nanourchin with different morphologies. Reprinted from ref. 176 with permission. Copyright (2011) American Chemical Society. Reprinted from ref. 122 with permission. Copyright (2010) Elsevier. Reprinted from ref. 20 with permission. Copyright (2012) Royal Society of Chemistry.

generate different morphologies or NP sizes, a growth solution (containing abundant metal salt, a weak reducing agent, and structure-decorating reagents) is added to a previously fabricated seed-mediated solution to produce rod-like shapes,[18] star shapes,[19] urchin-like shape,[20] tetrahedra,[21] nanoprisms,[22] obtuse triangular bipyramids,[23] *etc.* The selection of these NP structures depends on their applications. Thus, shape-controlled syntheses have become important.

The shape-controlled synthesis of metal NPs can be traced back to as early as the 1990s. Masuda *et al.* demonstrated Au nanorod (NR) synthesis using nanoporous aluminum oxide templates to reduce Au shaping.[24] Yu *et al.* developed a simple and high-quality Au NR synthesis route using quaternary ammonium surfactants by electrochemical oxidation.[25] Moreover, a well-known seed-mediated growth method was developed by Jana *et al.* to produce Au NRs with a controllable aspect ratio in high yield.[26] Au NPs with versatile morphologies can also be fabricated by a seeded-growth method.[27,28] Several approaches to the decoration of material morphologies have been proposed. The seed/Au salt ratio or other impurity ions in the solution direct the aspect ratio of Au NRs.[29] Addition of excess Au(I) to the solution tailors the optical properties and structures of the materials through the disproportionation reaction of Au(I) to generate Au(III) or Au(0).[30] Changing seed-mediated particles such as NRs also generates different morphologies.[31] Galvanic replacement is another well-known method for synthesizing hollow, skeleton, or cage structures of metal NPs.[32] Fig. 1 shows various shape-controlled metal nanomaterials.

2.2 Carbon-based NMs

Various NMs have been extensively investigated because of their special properties different from their bulk state.[33] Unlike other metal NPs, carbon-based materials in nanoscience are a special and new category in chemistry, physics, electronics, and materials. Members of the versatile allotrope of the carbon family include the fullerenes, carbon nanotubes (CNTs), graphene, graphite, nanodiamond, amorphous carbon, onions, horns, rods, cones, bells, foam, platelets, and peapods.[34] Nanodiamonds mainly have an sp^3-tetrahedral bond network confined in the nanoscale, and replacing the π electron network in another sp^2 plate forms carbon materials, such as tubes, graphene, graphite, and fullerenes, as shown in Fig. 2.[35]

Fullerenes (C_{60}) have an sp^2 carbon-based truncated icosahedral structure, as first reported by Kroto *et al.* in 1985. C_{60} has 12 pentagons and 20 hexagons, and an average diameter of around 7 Å.[36] Controlling the self-organization of pristine C_{60} by altering their dimensionality to adjust their structural,[37] magnetic,[38] electrochemical,[39] or photophysical[40] properties has drawn interest.

Several shape-controlled synthesis procedures are available for C_{60},[41] such as template-assisted, dip-drying, solution-driven, self-assembled, and vapor-driven crystalline methods.[42,43]

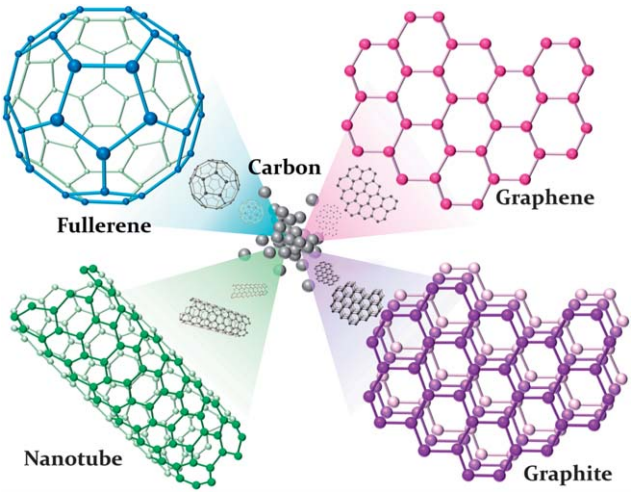

Fig. 2 Carbon allotropes in different structures.

Among them, the solvent-based, morphology-controlled synthesis of C_{60} has been widely investigated recently, and the shape of C_{60} can be tuned to NRs,[44] nanowhiskers,[45] nanosheets,[46] microtubes,[47] spheres, nanoballs,[48] *etc.* The different synthesis routes of various C_{60} morphologies are controlled by tailoring the crystalline structures.

CNTs were first documented in 1976 by Oberlin *et al.* CNTs are formed by rolling up graphene sheets of a single sp^2 layer and densely packing them such that diameters in the nanoscale and lengths in the microscale are achieved.[49] In 1991, Iijima observed multi-walled CNTs (MWCNTs), and became interested in CNT research over the next two decades.[50] Depending on the covering layer, CNTs can be classified into MWCNTs and single-walled CNTs (SWCNTs). Currently, the three main synthesis methods of CNTs are arc discharge, laser ablation, and chemical vapor deposition.[51] Compared with CNTs, SWCNTs are attracting more attention because of their outstanding electrical, mechanical, thermal, sensing, and optical properties that enable them to be utilized in many applications, such as chemistry, energy, electronics, optoelectronics, biomaterials, *etc.*[52]

The shape-controlled synthesis of NMs determines the physical or chemical properties of the materials. Diameter- or length-controlled SWCNT syntheses influence the physical and electronic properties of the resulting materials, as well as their optical and electronic applications. In different synthesis routes, the diameter-controlled synthesis conditions of SWCNTs are determined. In the arc discharge method, an alternative metal catalyst or chamber pressure controls the diameter range from 1.0 nm to 1.4 nm.[53] The change in furnace temperature between 780 and 1200 °C alters the diameter between 1.0 nm and 1.3 nm.[54] Additionally, the SWCNT diameter always increases with increased growth temperature. Sonication power is another controlling factor for changing the SWCNT length.[55] Controlling the diameter, length, concentration, and density of SWCNTs is important in a wide variety of applications.[56,57]

Graphene is another sp^2 carbon-based material with sheets arranged in a single-layer, hexagonal network. The discovery of monolayer graphene can be traced back to the 1960s and 1970s. In 2004, Novoselov *et al.* demonstrated the transfer of graphene onto silicon substrates and found an interesting electronic property.[58] The methods of synthesizing graphene are rapidly developing, including mechanical exfoliation,[58] nanotube unzipping,[59,60] chemical vapor deposition,[61,62] and oxidative exfoliation.[63,64] The properties of graphene are directed by different synthesis methods and determine the selection of applications in energy storage,[65] nanoelectronics,[66–68] or bio-applications.[69]

2.3 Semiconductor NMs

Fluorescent semiconductor NMs, also known as QDs, are powerful nanoscale light sources applied in various technologies. QDs are often made up of groups II and VI elements (*e.g.*, CdSe, CdTe, or ZnO) or group III and V elements (*e.g.*, InP). Nanosized semiconductors are gaining attention because of their interesting electronic and optical properties. The fluorescence range of QDs can be well tuned by changing their size or morphology based on the quantum confinement effect.[70] The band gap of QDs is inversely proportional to their size, *i.e.*, the fluorescence red shifts with decreased size. The tunable fluorescence property can be utilized in different applications, such as light-emitting diodes or bio-labeling.[71]

The synthesis of colloidal QDs can be traced back to the work of Murray *et al.* in 1993.[72] They demonstrated a high-temperature, organometallic system that processed nucleation and growth at high temperatures, and capped NPs with phosphor-based stabilizers. However, the unstable organometallic precursor they used, dimethyl cadmium, limited the synthesis of QDs with uniform morphology. To improve the quality of QDs, metal precursors have been tested, such as cadmium precursors (cadmium perchlorate, cadmium oxide, cadmium chloride, and cadmium carbonate).[73–75] Simple synthesis routes for uniform-sized or aqua-synthesized QDs are now available, and high-quality QDs can be obtained by altering the synthesis conditions, such as temperature, metal precursors, or capping ligands (Fig. 3).[76]

The shape-controlled synthesis of QDs has also been explored in recent decades. The anisotropic growth of QDs was discussed in 2000 by Peng *et al.*[77] A change in the capping ligand from pure trioctyl phosphine oxide (TOPO) to a mixture of TOPO and hexyl phosphonic acid (HPA) can adjust the growth rate and shape of nanostructures. At high concentrations of HPA, the reaction kinetics is altered and tends to produce rod-like QDs. The aspect ratio, size, and growth kinetics of these QDs can be systematically controlled by changing the reaction times, growth temperature, and number of injections. The seed-mediated growth of QDs has also been studied to produce rod-like or tetrapod structures.[78] This method can enable the selection of different materials from the seed and growth solution to fabricate core–shell structures.

3 Cellular uptake and intracellular trafficking of NMs

Given the size, unique optical property, and flexible surface modifications of NMs, they show great potential for various biomedical applications, including gene/drug delivery,

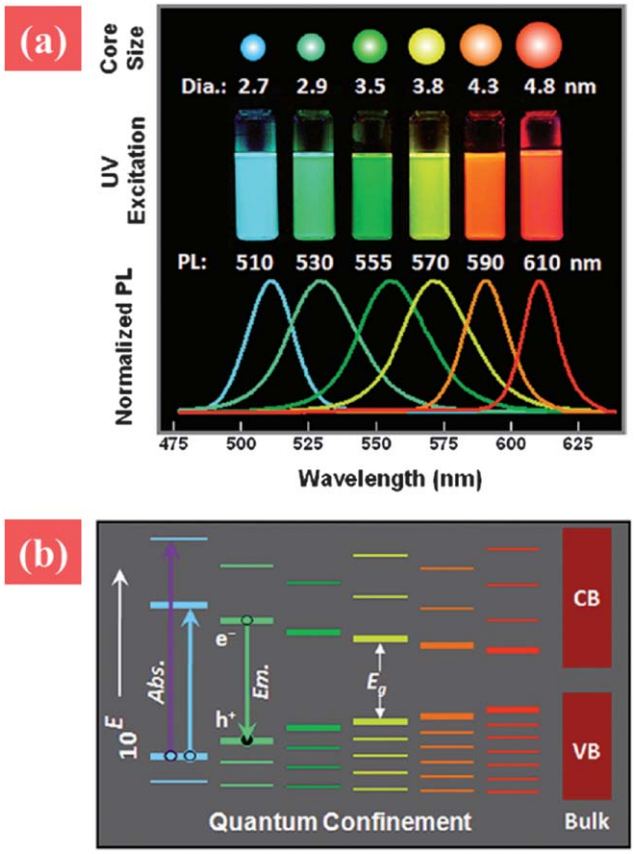

Fig. 3 (a) Photographs and photoluminescence spectra of quantum dots with various particle sizes, and (b) qualitative alternatives of quantum dots with increased particle size. Reprinted from ref. 12 with permission. Copyright (2011) John Wiley & Sons.

biosensing, bioimaging, and photothermal cancer therapy. For safety consideration in biomedical applications, a comprehensive understanding of the interactions between NMs and biological systems is needed, leading to the following questions. Do NMs enter cells? If they do, what kind of uptake pathway is involved? What intracellular organelles do NMs penetrate? What is the final fate of both NMs and cells? To answer these questions, different uptake inhibitors and state-of-the-art techniques such as transmission electron microscopy or confocal microscopy are used to study the internalization and cellular trafficking of NMs. Thus, to design NMs for specific biomedical purposes and elucidate possible hazardous effects, the mechanisms underlying the cellular uptake and intracellular trafficking process of NMs must be understood.

The uptake pathways include the clathrin-mediated, caveolae-mediated, and lipid raft-mediated endocytosis and phagocytosis, as well as pinocytosis and macropinocytosis. Phagocytosis is normally for specialized cells such as monocytes and macrophage. As shown in Fig. 4, these internalization pathways are involved in the cellular uptake of NMs.[79] Given their small size and protein adsorption in cell culture media, NMs are mostly consumed by cells through endocytosis, trapped into endosomes, transferred to lysosomes, and then excluded out of cells. However, some NMs can get out of endosomes and enter other organelles such as cytosol, mitochondrion, and even nucleus. In the following section, we discuss the most widely studied NMs as examples to show their typical cellular uptake and intracellular trafficking.

3.1 Noble metal-based NMs

3.1.1 Au NMs. Au NMs and their interactions with cells have been extensively studied in recent years for biomedical applications. Most reports indicate that Au NMs are taken up by receptor-mediated endocytosis, and are located in endosomes/lysosomes without entering mitochondria or nuclei.[80–83] For example, Chithrani *et al.* studied the cellular uptake and transport of Au NPs in breast cancer cells (MCF-7).[80] Results show that Au NPs are internalized through receptor-mediated endocytosis and trapped into endosomes, which are then fused with lysosomes. However, different uptake pathways and

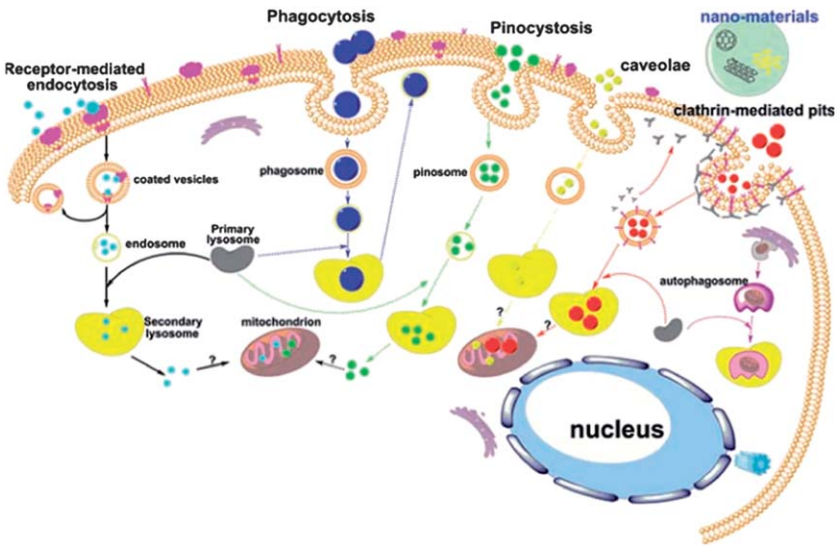

Fig. 4 Schematic of the known pathways for the intracellular uptake of NPs. Reprinted from ref. 79 with permission. Copyright (2011) John Wiley & Sons.

intracellular localization have been reported. For example, 60 nm Au NPs are internalized into murine macrophages by phagocytosis.[84] 3-Mercaptopropionic acid (MPA) and poly-(ethylene glycol) (PEG)-modified Au NPs (Au@MPA–PEG) are found in intracellular vesicles, cytoplasm, and nucleus in human cervical cancer (HeLa) cells.[85] After internalization and intracellular trafficking, the final fate of Au NMs is the next concern. Will they be excluded out of the cells or continue to stay in the cells and then gradually degrade? A study shows that Au NMs are excluded out of the cells in a time- and size-dependent manner.[83] Additionally, the intracellular trafficking and final fate of Au NMs are also cell type dependent. A study on Au NRs by our group indicates that the intracellular trafficking, including endocytosis and exocytosis, of Au NRs differs between normal and cancer cells, as shown in Fig. 5.[86] In normal lung epithelial (16HBE) and stem (MSC) cells, Au NRs are taken up by receptor-mediated endocytosis and located in endosomes/lysosomes, eventually being excluded out of cells. Meanwhile, in human lung cancer cells (A549), Au NRs are released from endosomes/lysosomes and enter the mitochondrion, which causes subsequent cell death.

In addition, the cellular uptake and trafficking of Au NMs are highly related to their size, shape, surface modification, and surface charge. Au NMs have high affinity for thiols, which provide a good chance for various surface modifications to facilitate their biomedical applications. For instance, targeted gene/drug delivery can be achieved by modifying Au NMs with a nuclear localization signal (NLS).[87,88]

3.1.2 Ag NMs. Ag NMs have broad antimicrobial activity; thus, they are widely used in a variety of commercial products, such as personal care products, paints, food storage containers, home appliances, laundry additives, *etc.*[89] However, the potential adverse effects of Ag NMs on human health and environmental safety are of concern. *In vitro* studies on the biological interactions of Ag NMs with cells have been performed, and Ag NMs can reportedly enter cells through endocytosis and translocate into endosomes/lysosomes, mitochondria, and nuclei.[90,91] For example, the intracellular localization of Ag NPs in human normal, bronchial, and epithelial (BEAS-2B) cells after 24 h exposure has been studied.[92] Results show that aggregated Ag NPs are located in endocytic vesicles within the cytoplasm and nucleus, suggesting an endocytic pathway for Ag

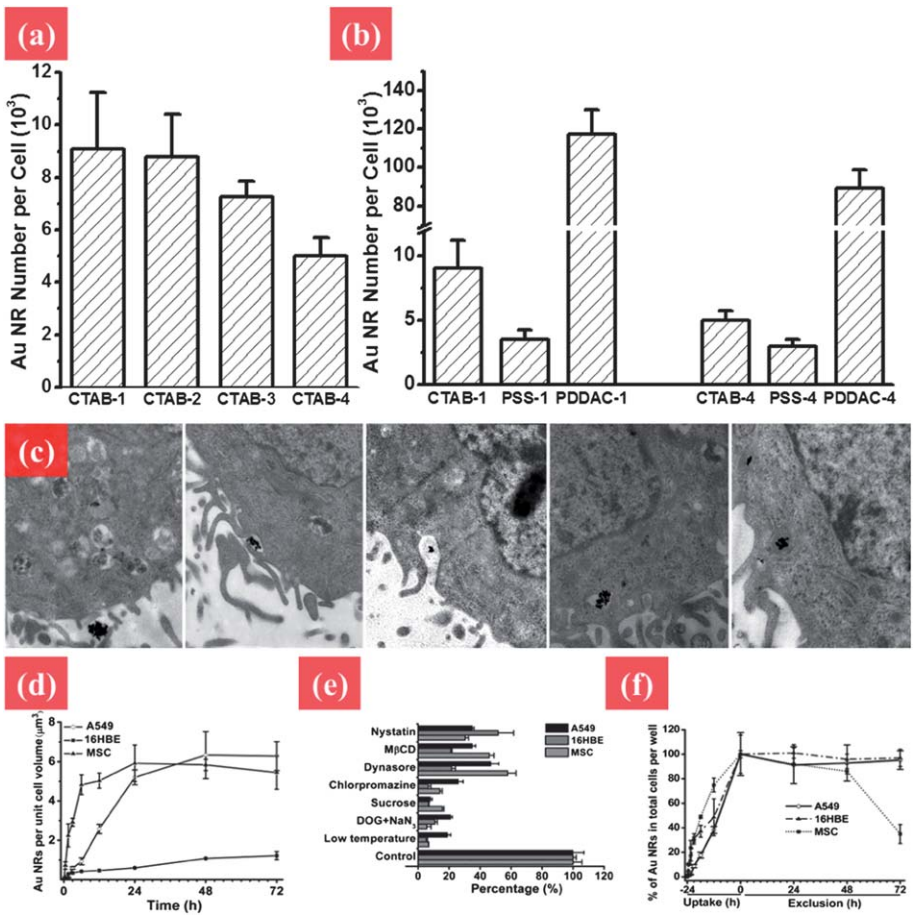

Fig. 5 Elucidating the mechanism of endocytosis and exocytosis of Au NRs with different surface chemistry and aspect ratios. (a) Cellular uptake of Au NRs by MCF-7 cells with different aspect ratios from 1 to 4: CTAB-1, CTAB-2, CTAB-3, and CTAB-4. (b) The shape and surface coating influencing cellular uptake of Au NRs. (c) TEM images showing the process of cellular uptake. The Au NRs form aggregates, enter into vesicles and further get into lysosomes. Uptake pathways and the quantitative process of internalization and removal of Au NRs in A549, 16HBE, and MSC cells by ICP-MS after treatment with 50 μM Au NRs. (d and e) Process of cellular internalization and exclusion of Au NRs, respectively. (f) Uptake pathways for Au NRs in three types of cells using specific endocytosis inhibitors. Reprinted from ref. 122 with permission. Copyright (2010) Elsevier. Reprinted from ref. 86 with permission. Copyright (2010) American Chemical Society.

NP internalization. However, the non-nuclear localization of Ag NPs has also been reported. Lina Wei *et al.* studied the uptake and intracellular distribution of Ag NMs in mouse fibroblast cells (L929).[93] They found that Ag NMs are phagocytized into cells, and localized in the endoplasmic reticulum and mitochondrion. The possible ability of Ag NMs to enter the cell nucleus remains to be clarified considering that Ag NMs are not as stable as Au NMs. Ag NMs may release Ag ions that are sufficiently small to enter any cell organelle, which may induce toxicity by interacting with protein or nucleic acid. In addition, the different surface chemistries of Ag NPs result in different behaviors of NPs in cells.[94] Uncoated Ag NPs agglomerate and may be excluded from the nucleus and mitochondrion, whereas polysaccharide-coated Ag NPs do not agglomerate and are distributed throughout the cell.

3.2 Carbon-based NMs

3.2.1 Fullerenes. Fullerenes (C_{60}) are carbon cages with nanoscaled three dimensions, which offer a unique scaffold for the covalent attachment of multiple drugs. However, the application of pristine C_{60} is limited by its insolubility in aqueous environments. Hence, the synthesis of derived, water-soluble, non-toxic C_{60} is of particular interest for cancer therapeutics. Different uptake pathways and intracellular localization of C_{60} and its derivatives have been reported in various cell types. Several studies have indicated that C_{60} can easily enter cells and locate in the nucleus in both normal and carcinoma cells,[95,96] which make them ideal agents for gene/drug delivery. Individual C_{60} molecules only have a diameter of 0.7 nm; thus, C_{60} may penetrate ion channels and diffuse through pores in the nuclear membrane. However, the non-nuclear localization of C_{60} derivatives has also been reported.[97] For instance, Wei Li *et al.* explored the uptake processes of $[C_{60}(C(COOH)_2)_2]_n$ NPs in 3T3, L1, and RH-35 living cells.[98] These derived C_{60} NPs are quickly internalized into cells by clathrin-mediated but not by caveolae-mediated endocytosis, and then synchronized to the lysosome without entering the nucleus. In another report, an amine-functionalized C_{70}–Texas Red conjugate is found to be internalized into cells by nonspecific endocytosis, and translocated to the cytoplasm, lysosome, mitochondrion, and endoplasmic reticulum of mast cells without entering the nucleus cells.[99] An accumulative assessment of the above reports suggests that the uptake and intracellular localization of derivatized C_{60} depend on the nature of their surface modifications and possibly on the type of the cell investigated. These observations warrant further study because of the possibility of targeting cancer cells or specific intracellular organelles of interest by C_{60} cage surface modifications.

3.2.2 CNTs. CNTs have elicited scientific interest because of their remarkable optical, mechanical, and electrical properties. As aforementioned, CNTs are classified into SWCNTs and MWCNTs.[100] Given their tubular structure and extremely high aspect ratio, CNTs can readily penetrate various biological barriers. Therefore, the behavior of CNTs in living cells, including cell entrance, subcellular locations, and excretion, is crucial for their effects on cellular functions. A popular view is that CNTs are taken up by cells through clathrin-dependent endocytosis. Although the majority of published data agree with the endocytosis model, energy-independent cell uptake has also been reported. Another controversy is on the subcellular locations of CNTs. CNTs can reportedly enter cells without entering the nucleus.[101,102] Other studies show that SWCNTs enter the cell nucleus[103–106] but this entry may be reversible.[106] Exocytosis of SWCNTs was observed and the rate closely matches the endocytosis rate with negligible temporal offset.[107] Mu *et al.* suggested an uptake model for MWCNTs based on their experimental results, *i.e.*, single MWCNTs enter cells through direct penetration, whereas bundles of MWCNTs enter cells through endocytosis.[108] However, MWCNT bundles in endosomes may release single nanotubes, penetrate the endosome membrane, and then escape into the cytoplasm. Short MWCNTs can also enter the cell nucleus. Finally, all classes of MWCNTs are recruited into lysosomes and excluded out of cells.

3.2.3 Pristine graphene and graphene oxide. Owing to their unique physicochemical properties, pristine graphene (PG) and graphene oxide (GO) have attracted tremendous research interest for potential applications in electronics, energy, materials and biomedical applications such as drug delivery, anticancer therapy, especially as scaffolds for tissue engineering.[109] Unlike fullerenes and CNTs, PG is not likely to be taken up by cells. For example, a comprehensive examination by Chang *et al.* indicated that GO was not internalized into A549 cells and negligible toxic effects were induced at low concentrations. However, Yue *et al.* examined the ability of six cells in the internalization of GO.[110] They found that phagocytes were the only cell type in their study that was capable of internalizing GO. Interestingly, the cellular uptake of GO is not size dependent. 2 μm and 350 nm of GO, which greatly differ in lateral dimensions, did not show much difference in the cellular uptake amount. However, the intracellular localization and subsequent biological effects are size dependent. The GO in micro-size showed divergent intracellular locations and induced much stronger inflammation responses. In addition, the difference in biological effects between PG and its functional derivatives was compared in monkey kidney cells, Vero.[153] PG was found to accumulate on the surface of the cell membrane, which induces high oxidative stress and consequently apoptosis, whereas carboxyl functionalized hydrophilic graphene was internalized by the cells without causing any toxicity. Conclusively, the surface modification and cell type are of critical importance when evaluating the interactions between PG and GO with cells, which should be carefully considered for safe biomedical applications.

3.3 Semiconductor NMs

QDs show promising properties as an alternative fluorophore to organic dyes for biological labeling and bioimaging. With their strong fluorescence intensity, photostability, small size, and flexible surface modifications, QDs are ideal agents for intracellular tracking based on *in vitro* and *in vivo* studies. Therefore, concern on the fate of QDs in biological systems is growing. For

example, the cellular uptake of QDs into human epidermal keratinocytes has been explored.[111] Results indicate that carboxylic acid-coated QDs composed of a cadmium/selenide core and a zinc sulfide shell are taken up by cells through the G-protein/coupled-receptor-mediated pathway and low-density lipoprotein receptor/scavenger receptor-mediated endocytosis. These QDs are subsequently internalized into early endosomes and then transferred to late endosomes/lysosomes without entering the cell nucleus. Tat-QDs were found to be trapped in vesicles and remain tethered to the inner vesicle membranes inside the cytoplasm, then the QDs-loaded vesicles were transported to a perinuclear region called the microtubule organizing center (MTOC).[112] Interestingly, vesicles containing large QDs pinch off from the tips of filopodia, resulting in free vesicles with Tat-QDs bound on the outside.[112] A study has shown that cell nucleus localization may be size dependent.[113] Red QDs are distributed throughout the cytoplasm of N9 cells but do not enter the nucleus, whereas green QDs predominantly localize in the nucleus. Thus, the size of pores in the nucleus plays an important role in the nucleus localization of NMs. Another study has shown that the cellular uptake of QDs depends on the cell type and cell differentiation;[114] the ability for QD655-COOH cellular uptake is found in monocytes but not in lymphocytes. However, monocyte differentiation into dendritic cells increases the cellular uptake of QD655-COOH by sixfold. In addition, different surface modifications can be used to facilitate QDs uptake for intracellular tracking application.[112,115] For example, QD surfaces modified with dihydrolipoic acid or PEG attached onto a polyethylenimine coating can be taken up into human cells by endocytosis and then translocated into the cytoplasm.[116,117] Overall, the cellular uptake and intracellular localization of various NMs somewhat depend on the size, shape, surface modification, and cell type.

4 Potential toxicity induced by nanostructured materials

Recent advances in engineering and technology have led to the development of many new NMs. Gathering information on the potential hazardous effects of these NMs on human health and environmental safety is becoming urgent. Given their size and large surface area, NMs are much more active than their bulk counterparts. Upon exposure, NMs can easily enter cells by direct penetration or receptor-mediated endocytosis, and are then translocated into different organelles. The NMs may then interact with intracellular components such as proteins, lipids, or nucleic acids. Production of increased reactive oxygen species (ROS) is considered as the most common pathway for NMs induced toxicity. High ROS levels are indicative of oxidative stress, and can damage cells by peroxidizing lipids, inducing inflammation, altering proteins and DNA, as well as interfering with signaling and gene functions.

4.1 Noble metal-based NMs

4.1.1 Au NMs. The interactions of Au NMs with different cells, including fibroblasts of the human skin (HeLa), human lung carcinoma (A549), human hepatocarcinoma (HepG2), human breast carcinoma (MCF7), *etc.*, have been studied. However, the results on their toxicological issues are still controversial. Most studies show that Au NMs are biocompatible and have negligible toxicity. Au NMs are adsorbed with proteins immediately after introduction to serum containing a cell culture medium. The particle–protein complex is then taken up by cells and localized in endosomes/lysosomes in most cases. A small amount of Au NMs induces cytotoxicity if they do not enter the cytoplasm or nucleus. For example, 60 nm Au NPs have been internalized by murine macrophages without causing cytotoxicity or producing pro-inflammatory mediators.[84] However, many studies show the cytotoxicity effects of Au NMs.[118–120] Notably, in most cases, the toxicity of Au NMs originates from their surface properties, such as their surface charge and surface molecules, and not from the Au NMs themselves.[121] Our group has studied the cytotoxicity of Au NRs with different surface modifications (including cetyltrimethylammonium bromide (CTAB), polystyrene sulfonate (PSS) and poly(diallyldimethylammonium chloride) (PDDAC)) to MCF-7 cells, as shown in Fig. 5.[122] Results show that CTAB-coated Au NRs are much more toxic than the PSS- or PDDAC-coated ones. The possible reason is that free CTAB released from the Au NR surface coating and also from the stock solution damages the membrane integrity of endosomes/lysosomes and mitochondria, leading to increased intracellular ROS production and eventual cell death. Additionally, the size and shape also have vital effects on their toxicity. Proper design of physicochemical properties of Au NMs should be considered for safe biomedical applications.

4.1.2 Ag NMs. Wide applications of Ag NMs in commercial products, particularly in wound dressing, increase the risk of Ag NMs entering tissues, cells, and biological molecules in the human body. Therefore, their adverse effects on human health are becoming more critical than ever. Studies on the toxic effects of Ag NMs on cells have been performed. Results showed that Ag NMs can induce oxidative stress, cell cycle arrest, inflammation reactions, chromosome aberration, and DNA strand breaks.[91,123,124] A number of studies have proposed that the induction of ROS is a general mechanism of NMs-mediated cytotoxicity which is supported by other studies showing that *in vitro* exposure to Ag NPs causes reduction in GSH, elevated ROS levels, lipid peroxidation, and increased expression of ROS responsive genes.[125–127] The Ag NPs-mediated increase in ROS is also associated with DNA damage, apoptosis, and necrosis.[125,127,128]

The mechanism underlying the toxicity of Ag NMs has been investigated. Binding of Ag ions to SH groups in proteins is suggested to be the mechanism behind the well-known antibacterial effect of Ag.[129] The toxic effects of Ag NPs can theoretically be related to the release of free Ag ions. There had been a discussion about which component contributes most to the toxicity of Ag NMs, the Ag NMs themselves or Ag ions being released. Two recent studies tested the content of free Ag ions in Ag NP solutions and found low levels of Ag^+ (0–1%). Furthermore, both studies concluded that the toxicity of Ag NPs exposure cannot be explained solely by the presence of Ag ions in the

NP solution.[127,130] Christiane Beer also suggested that both Ag NPs and Ag ions contribute to the toxicity of Ag NP solution.[131] Consequently, the question remains whether Ag NPs are intrinsically toxic or they act in a Trojan-horse like mode that enables uptake of the NPs and subsequent liberation of ions inside the cell.

4.2 Carbon-based NMs

4.2.1 Fullerenes. The toxicity of C_{60} is of particular concern because individual C_{60} molecules have a diameter of only 0.7 nm. They are therefore sufficiently small to enter cells through passive diffusion and diffuse through pores in the nuclear membrane. Researchers demonstrated that uncoated C_{60} can form aqueous suspended colloids (nano-C_{60}), which are redox-active and produce oxidative damage in the brain of a largemouth bass.[132] With its widespread application, studying the cytotoxicity of C_{60} is thus necessary. Several studies showed that C_{60} decreases cell growth and cell viability, and induces micronucleus in CHO, HeLa, and HEK293 cells in low doses and long term exposure.[133] It has been hypothesized that the cytotoxicity of C_{60} is related to its ability to cause oxidative stress. Christie M. Sayes *et al.* studied the cytotoxic mechanism of nano-C_{60} in human dermal fibroblasts, human liver carcinoma cells (HepG2), and neuronal human astrocytes.[134] Results show that nano-C_{60} is cytotoxic to all these three cell types after 48 h exposure. Further study showed that lipid peroxidation and the resultant membrane damage are responsible for the cytotoxicity of nano-C_{60} and the oxidative damage and resultant toxicity of nano-C_{60} are completely prevented by the addition of L-ascorbic acid as an antioxidant. The cytotoxicity of C_{60} can be reduced by appropriate surface modifications. The lethal dose of fullerene changed over 7 orders of magnitude with relatively minor alterations in fullerene structure.[135] In particular, an aggregated form of C_{60}, the least derivatized of the four materials, is substantially more toxic than highly soluble derivatives such as C_3, $Na_{2-3}{}^{+}[C_{60}O_{7-9}(OH)_{12-15}]^{(2-3)-}$, and $C_{60}(OH)_{24}$. Oxidative damage to the cell membranes is observed in all cases where fullerene exposure led to cell death. Under ambient water conditions, fullerenes can generate superoxide anions and these oxygen radicals are responsible for membrane damage and subsequent cell death.

4.2.2 CNTs. Given their remarkable optical, mechanical, and electrical properties, CNTs have been proposed for biomedical applications such as cell tracking and labeling, tissue engineering scaffolds, nanosensors, and vehicles for controlled release of drugs or delivery of bioactive agents. Detailed information about their biosafety is required for safe biomedical applications. Several *in vitro* and *in vivo* studies found significant cytotoxicity, DNA damage, micronucleus induction, or mutagenicity trends produced by carbon black or carbon-rich particles.[136–138] For example, MWCNTs can activate NF-κB, enhance phosphorylation of MAP kinase pathway components, and increase production of proinflammatory cytokines in human bronchial epithelial cells.[139] However, Zhong *et al.* showed that carbon black did not induce changes in DNA migration in V79 or Hel 299 cells.[140] Carboxylated MWCNTs did not significantly affect cellular morphology and viability of PC12 cells at lower concentrations. Moreover, short MWCNTs promoted neuronal differentiation of PC12 cells.[141] In summary, surface chemistry, physical properties, and dose are important factors in determining toxicity of CNTs. For example, CNTs can be readily taken up by cells and are noncytotoxic with appropriate surface modification and certain limit concentration.[104,142,143]

The reported underlying mechanisms are also controversial. As shown in Fig. 6, CNT-induced oxidative stress is regarded as the main toxic mechanism.[144–146] Conversely, Fenoglio *et al.* demonstrated that MWCNTs exhibited a remarkable scavenging capacity against an external source of hydroxyl or superoxide radicals.[147] In addition, iron impurity of CNTs is considered as another important reason for CNTs' toxicity.[148] Complications arise when comparing these investigations as there are often considerable variations in the methodologies used including differences in exposure protocols and duration, and length and frequency of post-exposure sampling. More importantly, pristine CNTs are highly hydrophobic, whereas surface functionalization (carboxylation, amination, or PEGylation) renders hydrophilicity and dispersibility in the aqueous phase, enabling varied interactions with biological systems.[149,150] Further extensive *in vitro* and *in vivo* investigation is necessary to arrive at more definitive conclusions about the genotoxic properties of CNTs and the possible mechanisms involved in such toxicity.

4.2.3 Graphene. PG and GO are two dimensional carbon-based NMs with single atom thickness. Given their large surface area and unique optical property, PG and GO are potential candidates for biomedical applications, such as gene/drug delivery[151] and phototherapy.[152] For safe biomedical applications, biocompatibility studies on graphene-related NMs are needed.

The toxicity of graphene and its derivatives to bacteria and cells have been studied. For example, GO and reduced GO (rGO) can inhibit bacterial growth while causing minimal toxicity to human alveolar epithelial A549 cells.[153] However, the cytotoxicity of graphene and its derivatives is still without consensus. For example, PG and GO induce cytotoxic effects on phaeochromocytoma (PC-12) cells and human fibroblast cells.[138,154] However, two other recent reports indicated that PG and GO are quite biocompatible.[155,156] For example, PG and GO substrates are highly biocompatible with improved gene transfection efficiency in NIH-3T3 fibroblasts.[154] A possible explanation for this discrepancy is that the physicochemical properties of PG and GO, including size, surface charge, and surface functional groups, are not always well controlled, which may have significant influence on toxicological effects.[157] For example, Sasidharan *et al.* compared the cytotoxicity of PG and surface functionalized graphene; they found that PG accumulates on the monkey kidney cell membrane, causing high oxidative stress and subsequent apoptosis, whereas carboxyl functionalized hydrophilic graphene taken up by cells does not result in any toxicity.[158] For further toxicology study, as shown in Fig. 7, the underlying mechanism of the cytotoxicity of graphene has been studied.[159,160] Li *et al.* reported that PG induces cytotoxicity

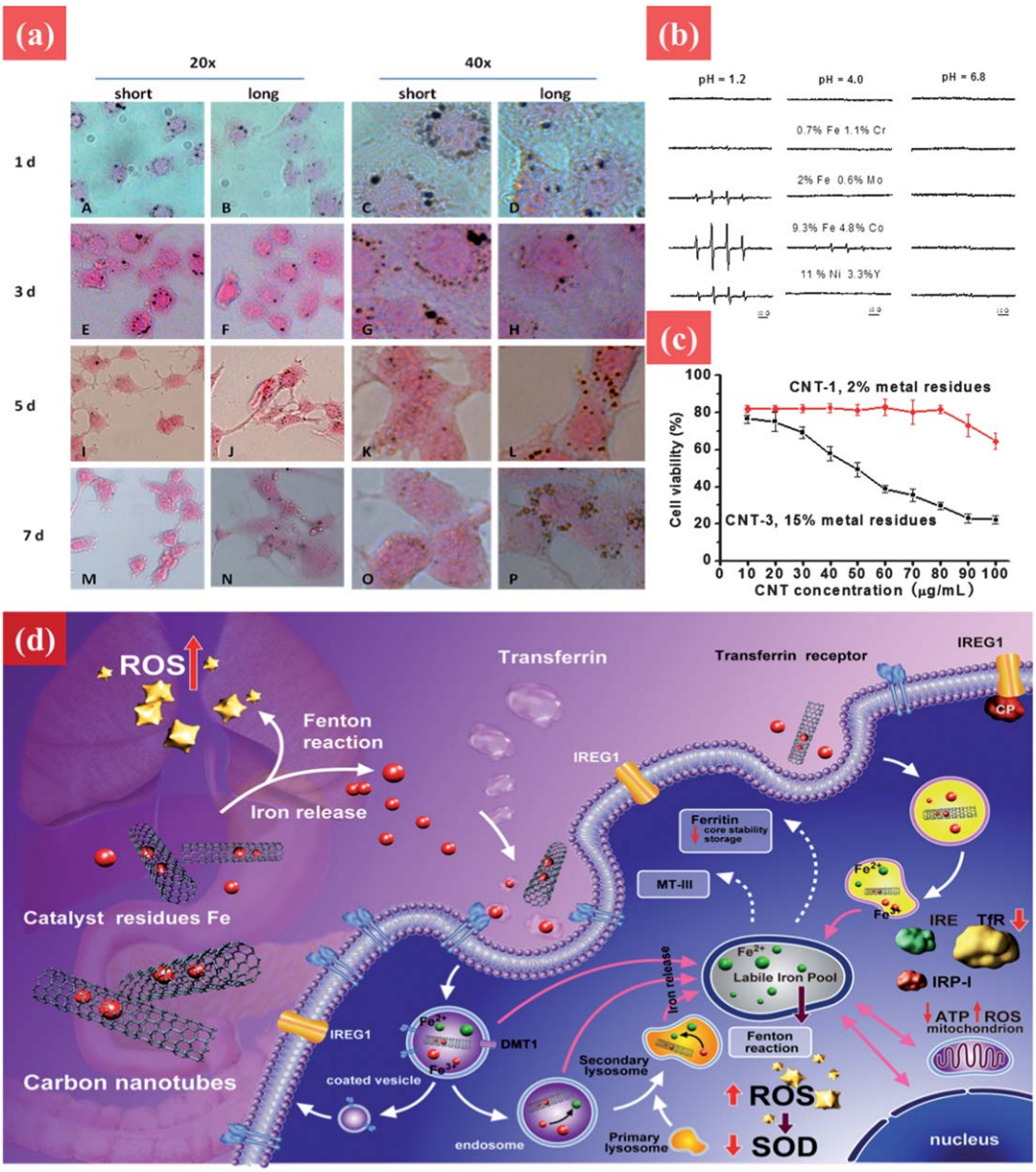

Fig. 6 The toxic effect of CNTs to cells and underlying mechanism. (a) Rapid transport of MWCNTs in PC12 cells. The cellular uptake and rapid removal of short MWCNTs at different time points were tested by HE staining during exposure to MWCNTs (30 μg ml^{-1}) for 2 days following culture in fresh medium in the absence of MWCNTs for 5 days. Cell images were taken at 1, 3, 5, and 7 days, respectively. (b) Hydroxyl radical formation from nanotubes having different metal contents at different pHs. (c) The cell viability after treatment with CNTs with different iron impurities. (d) Transport pathway, cellular and molecular mechanisms of toxicity associated with cellular exposure to carbon nanotubes and leached metal. Reprinted from ref. 145 with permission. Copyright (2012) Nature. Reprinted from ref. 146 with permission. Copyright (2013) John Wiley & Sons.

in macrophages through the depletion of the mitochondrial membrane potential (MMP) and the increase of intracellular reactive oxygen species (ROS), then triggers apoptosis by activation of the mitochondrial pathway.[159] However, at a lower concentration, graphene significantly stimulates the secretion of Th1/Th2 cytokines including IL-1α, IL-6, IL-10, TNF-α and GM-CSF as well as chemokines such as MCP-1, MIP-1α, MIP-1β and RANTES, probably by activating TLR-mediated and NF-κB-dependent transcription. This feedback of the immune response of macrophages by graphene-induced factors may play an important role in the prevention of their over-activation after graphene exposure.[160]

4.3 Semiconductor NMs

QDs are of special interest because of their potential application as fluorescent probes for bioimaging and diagnostics. However, before QDs can be used safely *in vivo*, more information about their interaction with and potential toxicity to biological systems is needed. The toxicity of QDs has been studied in a large number of *in vitro* studies.[113,114,161,162] Results showed that exposure to QDs affects cell growth and viability. The extent of cytotoxicity depends on a number of factors including composition, size, and surface capping materials.[113,163,164] The possible reasons for the toxicity of QDs are

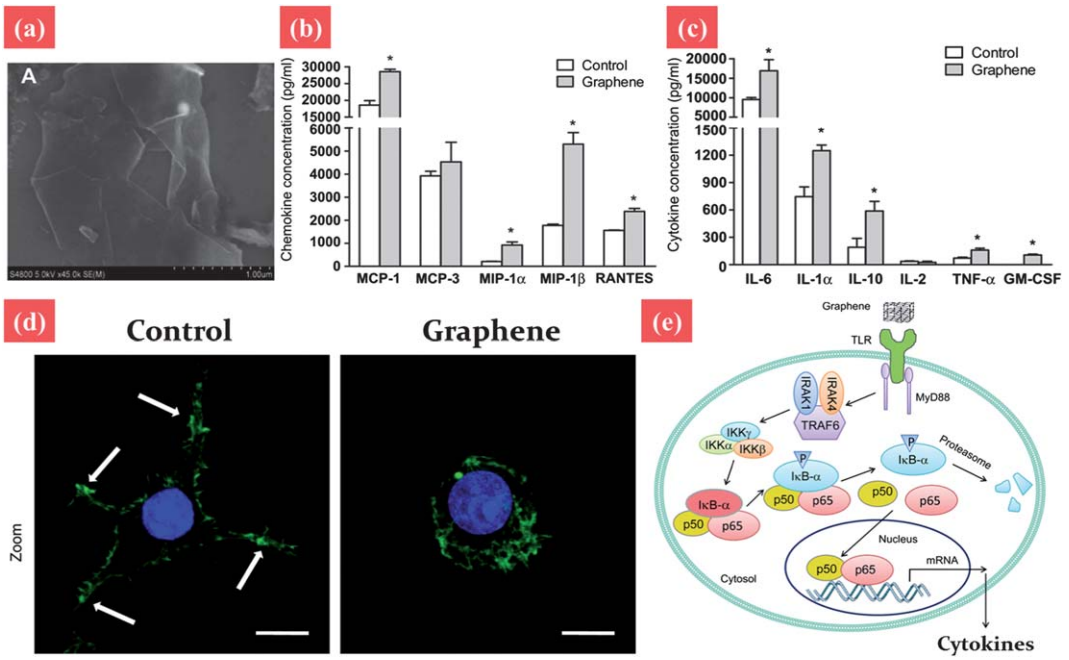

Fig. 7 Signaling the pathway of macrophage activation stimulated by graphene nanosheets. (a) The SEM image of pristine graphene nanosheets. (b and c) Graphene nanosheets stimulate the secretion of cytokines and chemokines in macrophages. (d) Actin cytoskeleton of macrophages. The arrows indicate the F-actin foci of podosomes. (e) Graphene may be recognized by certain types of TLRs, thus activating kinase cascades by a MyD88-dependent mechanism. Activation of IKK initiates the phosphorylation and consequent degradation of IkB, resulting in the release of NF-κB subunits, and their translocation into the nucleus. NF-κB binds to the promoter regions of its effector genes, and initiates the transcription of multiple proinflammatory genes and the secretion of various proinflammatory factors, including IL-1α, IL-6, IL-10, TNF-α, CM-CSF, MCP-1, MIP-1α, MIP-1β and RANTES. These proinflammatory factors modulate the immune responses of neighboring macrophages. Reprinted from ref. 159 with permission. Copyright (2012) Elsevier. Reprinted from ref. 160 with permission. Copyright (2012) Elsevier.

discussed, including desorption of free Cd (QD core degradation),[163] free radical formation, and interaction with intracellular components. However, studies demonstrated that correct capping and improved surface coating of QDs can minimize cytotoxicity arising from air and photo-oxidation. Several synthesis, storage, and coating strategies have been developed for QDs to ensure stability of these NPs and minimize toxicity.[74,164,165] In addition, cellular uptake plays an important role in NMs toxicity. Chang *et al.* evaluated the toxicity of surface coated QDs based on intracellular uptake and demonstrated that the improved biocompatibility of PEG coated QDs compared with bare ones is because of the decreased cellular uptake through endocytosis.[161] Therefore, the cellular uptake of NMs directly affects their toxicity, not their surface modification.

In addition, it is important that the cytotoxicity evaluation assays that are being used are appropriate for the materials being tested. For example, in the neutral red assay, carbon black has been shown to adsorb neutral red dye molecules which can give false positive results.[166] Regarding the toxicology of NMs, it is difficult to draw conclusions because of the different experimental systems, including cell types, NMs compositions, exposure strategies, and toxicity evaluation systems in various laboratories. Therefore, to compare results from different labs, it is highly essential to include all the information referring to NPs characterization, exposure strategy, and toxicity evaluation systems in the published paper.

5 Major factors influencing the biological effects of nanostructured materials

The interaction between NMs and cells has been considered in recent studies because the physical and chemical properties of NMs strongly influence the biochemical properties of cells while they are in contact with each other. The physical and chemical properties include physical factors (size, shape, surface area, and surface compositions), surface chemistry (surface charge, surface functionalization and whether the NM is hydrophobic or hydrophilic), and physiological stability (aggregation, agglomeration, biodegradability, and solubility). In nature, physicochemical properties are crucial to the physiology of cells, including uptake properties (ratio, amount, and mechanism), transportation properties (accumulation location and transportation process), cytotoxicity (necrosis, apoptosis, and decreased cell viability), and exclusion. Owing to interaction between NMs and cells, these effects and behaviors should be seriously considered before being applied to any additional biological systems. Certain physicochemical parameters of NMs affect the physiological interactions of cells, as shown in Table 1.

5.1 Effects of NM size

The size of NMs strongly affects their optical properties, as discussed in the previous section. However, NM size is also crucial to physiological interaction. NMs have six size-dependent

Table 1 Parameters of the metal, carbon, and semiconductor-based nanomaterials in various cell lines

Category	Material	Characterization	Cell type	Exposure	Uptake pathway	Intracellular localization	Method	Toxicity	Ref.
Metal	Au	Au NPs, 60 nm	Murine macrophage cells	0.1–100 μg ml^{-1}; 24 and 48 h	Endocytosis	Endosomal vacuoles	MTT, LDH, ELISA, flow cytometry, transmission electron microscopy (TEM), EDX	No cytotoxicity and no elevated production of pro-inflammatory mediators	84
Metal	Au	Au NRs; CTAB capped; length: 55.6 ± 7.8 nm, width: 13.3 ± 1.8 nm	Lung carcinoma cells (A549), normal bronchial epithelial cells (16HBE), and primary adult stem cells (MSC)	25–200 μM; 24, 48, and 72 h	Clathrin and lipid raft-dependent (dynamin-mediated) endocytosis	Endosomes/lysosomes of 16HBE cells and stem cells, endosomes/ lysosomes and mitochondria in A549 cells	CCK-8, confocal microscopy, flow cytometry, ICP-MS, TEM	Kill cancer cells while posing negligible impact on normal cells and stem cells	86
Metal	Au	Au NRs; CTAB, PDDAC, PSS capped; aspect ratios 1.1, 2, 3, 4	Human breast adenocarcinoma cell line (MCF-7)	70 pM; 6, 12, 24, and 72 h	Receptor mediated endocytosis	Endosomes/lysosomes, mitochondria	CCK-8, confocal microscopy, flow cytometry, ICP-MS, TEM	Free CTAB in CTAB coated Au NRs decreases cell viability, damages mitochondrial membrane, increases ROS level and induces apoptosis	122
Metal	Au	PEG-Au NPs, 16 nm; PEG-Au NPs modified with cell penetrating peptides (CPPs) and nuclear localization signal peptide (NLS)	Human fibroblast cells (HeLa cells)	5 nM; 2 h	Clathrin and caveolae dependent endocytosis, cell penetration	Endosomes, cytosol, nuclei	TEM, atomic emission spectroscopy (AES)	NM	87
Metal	Au	Au NPs, 3.7 nm, Au@MPA–PEG, Au@MPA–PEG–FITC	Human cervical cancer (HeLa) cells	0.08, 0.313, 1.25, 2.5, 5 and 10 μM; 6, 12, 24, 36, 48 and 72 h	NM	Vesicles, cytoplasm, nuclei	Confocal laser scanning microscopy (CLSM), TEM, ICP-MS	Au NP@MPA–PEG did not induce obvious cytotoxicity	85
Metal	Ag	Spherical, mean diameter 46 ± 21 nm	Human mesenchymal stem cells (hMSCs)	0.01–10 μg ml^{-1}; 1, 3, and 24 h	Endocytosis as well as diffusion	Vesicles, cytoplasm, and nucleus	Trypan blue exclusion test, comet assay and chromosomal aberration test, ELISA, TEM	Decrease cell viability, induce DNA damage, increase of IL-6, IL-8, and VEGF release	90
Metal	Ag	Ag NPs, 43–260 nm	Normal human lung bronchial epithelial cells (BEAS-2B)	0.01–10 μg ml^{-1}; 24 h	Endocytosis	Endocytic vesicle within the cytoplasm and nucleus	TEM, comet assay, micronucleus assay, flow cytometry	Increase ROS, DNA damage and chromosome aberration	92

Table 1 (*Contd.*)

Category	Material	Characterization	Cell type	Exposure	Uptake pathway	Intracellular localization	Method	Toxicity	Ref.
Metal	Ag	Ag NPs, 25 nm, polysaccharide coated or not	Mouse embryonic stem (mES) cells, mouse embryonic fibroblasts (MEF)	50 μg ml^{-1}; 24, 48, and 72 h	NM	Uncoated Ag NPs agglomerate while the polysaccharide coated Ag NPs do not agglomerate and are distributed throughout the cell	Annexin V protein expression and MTT assay	Upregulated the cell cycle checkpoint protein p53 and DNA damage repair proteins Rad51 and phosphorylated-H2AX expression, induced cell death, coated Ag NPs exhibited more severe damage than uncoated Ag NPs	94
Metal	Ag	PVP-coated Ag NPs	A549 human lung carcinoma epithelial-like cell	1–15 μg ml^{-1}; 0–24 h	NM	NM	MTT, annexin V/ propidium iodide assays, atomic absorption spectroscopy, flow cytometry, ^{32}P-postlabeling	Dose-dependent cellular toxicity and genotoxicity which can be inhibited by antioxidants	124
Metal	Ag	Ag NPs, 6–20 nm, starch surface coating	Normal human lung fibroblast cells (IMR-90) and human glioblastoma cells (U251).	0–100 μg ml^{-1}; 24, 48, and 72 h	Endocytosis	Lysosomes, mitochondria, nucleus and nucleolus	ATP assays, DCF-DA and DHE staining, CellTiter Blue viability assay, flow cytometry, single cell gel electrophoresis (SCGE) and cytokinesis blocked micronucleus assay (CBMN), TEM	Interruption of ATP synthesis, production of ROS, cell cycle arrest in the G2/M phase, DNA damage	215
Carbon	SWCNTs	Ammonium-functionalized single-walled carbon nanotubes (SWNTs-NH_3^+)	Human Caucasian lung carcinoma (A549) and Chinese hamster ovary (CHO) cells	5–500 μg; 2 h	NM	Perinuclear	Confocal laser scanning microscopy (CLSM), flow cytometry	Absence of toxic effects	101
Carbon	MWCNTs	Multi-walled carbon nano-tubes diameter of 40–100 nm, 600–800 nm in length; and three kinds of carbon blacks, PG, S160, and P90 sized 51, 20, and 14 nm, respectively	HeLa cells	0.1–100 μg ml^{-1}; 2 h	Endocytosis	Endosome	MTT, optical microscopy, TEM	Cytotoxicity, MDA level of lipid peroxidation product increase and SOD reactivity decrease; a greater toxicity was observed in cells exposed to CNPs in the medium without serum compared with cells in the medium with serum	216

Table 1 (*Contd.*)

Category	Material	Characterization	Cell type	Exposure	Uptake pathway	Intracellular localization	Method	Toxicity	Ref.
Carbon	MWCNTs	MWCNTs, mean diameter, 67 nm; surface area, 26 m^2 g^{-1}; carbon purity, 99.79 wt%	BEAS-2B, a human bronchial epithelial cell line, transiently transfected CHO-KI cells	1–10 μg ml^{-1}; 0–24 h	NM	NM	WST-8, SEM, RT-PCR, western blot, reporter gene assay	MWCNT activated NF-κB, enhanced phosphorylation of MAP kinase pathway components, and increased production of pro-inflammatory cytokines in human bronchial epithelial cells	139
Carbon	MWCNTs	Carboxylated (MWCNT–COOH) and aminated (MWCNT–NH_2) CNTs	Human embryonic kidney epithelial cells (HEK293)	100 μg ml^{-1}; 1 and 48 h	Single MWCNTs enter cells through direct penetration while MWCNT bundles enter through endocytosis	Endosomes, cytoplasm, nucleus, and lysosome	TEM, flow cytometry	NM	108
Carbon	Fullerene	C_{60}, individual particles are 60–270 nm and the diameters of clusters are 420–1300 nm	Mature human macrophages	0–10 μg ml^{-1}; 24 and 48 h	Phagocytosis of larger aggregates or by endocytosis	Secondary lysosomes, along the outer and nuclear membrane and inside the nucleus	Neutral red assay, energy-filtered transmission electron microscopy (EFTEM), and scanning transmission electron microscopy (STEM)-based electron tomography	Concentrations of C_{60} used in this study are not toxic	95
Carbon	Fullerene	Nano-C_{60}	Human dermal fibroblasts, human liver carcinoma cells (HepG2), and neuronal human astrocytes	48 h	NM	NM	MTT, live/dead staining, LDH release, fluorescence microscopy, spectro-fluorometry	Decrease cell viability, damage membrane integrity; however, DNA concentration and mitochondrial activity are not affected	131
Carbon	Fullerene	Fullerenes (C_{70})	Human skin, tryptase–chymase positive MC (MCTC) type cells	5 μg ml^{-1} of C_{70}–TR; 5 h, washed, and photodocumented, or placed back in the culture for up to 1 week at 37 °C in a 6% CO_2 incubator	Endocytosed	Cytoplasm, lysosomes, mitochondria, and endoplasmic reticulum; no nuclear or secretory granule localization was observed	Confocal microscopy	Calcium and reactive oxygen species production	99

Table 1 (*Contd.*)

Category	Material	Characterization	Cell type	Exposure	Uptake pathway	Intracellular localization	Method	Toxicity	Ref.
Carbon	Fullerene	C_{60}, C_3, $Na_{2-3}^{+}[C_{60}O_{7-9}(OH)_{12-15}]^{(2-3)}$, and $C_{60}(OH)_{24}$	Human skin (HDF) and liver carcinoma (HepG2) cells	0.24–2400 ppb; 48 h	NM	NM	Live/dead viability/ cytotoxicity kit, LDH, MTT	Oxidative damage to the cell membranes and subsequent cell death. C_{60} was substantially more toxic than the other three derivatives	135
Carbon	Fullerene	$C_{60}(C(COOH)_2)_2$	HeLa and Rh35 cells	0.01, 0.1, 1, 10, 100 mg l^{-1}; 24 h	Endocytosis or other pathways	Cytoplasm	Fluorescence microscopy, flow cytometry	Concentrations ranging from 1×10^{-2} to 1×10^{2} mg l^{-1}, $C_{60}(C(COOH)_2)_2$ does not show any detectable cytotoxicity	97
Carbon	Graphene	Graphene oxide	Human fibroblast cells	5, 10, 20, 50, and 100 μg ml^{-1}; 5 days	Endocytosis	Lysosomes, mitochondrion, endoplasm, and cell nucleus	CCK8, spectrophotometry, western blot, TEM	A dose less than 20 μg ml^{-1} does not exhibit toxicity; a dose above 50 μg ml^{-1} exhibits obvious cytotoxicity, decreasing cell adhesion and induces cell apoptosis	154
Carbon	Graphene	Pristine graphene, carboxyl functionalized hydrophilic graphene	Vero cells	0–300 mg ml^{-1}; 24 h	NM	Pristine graphene was found to accumulate on the cell membrane, carboxyl functionalized hydrophilic graphene was internalized by the cells	Confocal and flow cytometry, cell viability and LDH leakage	Pristine graphene causes high oxidative stress leading to apoptosis, whereas carboxyl functionalized hydrophilic graphene causes no toxicity	158
Carbon	Graphene	Graphene- and carbon nanotube-coated substrates	NIH-3T3 fibroblast cells	24 h and 48 h	NM	NM	Live/dead assay, RT-PCR, fluorescence microscopy	High biocompatibility, enhance gene transfection efficiency	155
Semi-conductor	QDs	Cadmium/selenide core with a zinc sulfide shell, carboxylic acid surface coating	Human epidermal keratinocytes (HEKs)	2 nM; 2, 6, 12, and 24 h	Lipid rafts mediated endocytosis	Early endosomes and then transferred to late endosomes or lysosomes	TEM, confocal microscopy, flow cytometry, spectrofluorometry	The low toxicity of QDs was shown with the 20 nM dose in HEK at 48 h, but not at 24 h by the live/dead cell assay. QDs induced more actin filaments formation in the cytoplasm	111

Table 1 (*Contd.*)

Category	Material	Characterization	Cell type	Exposure	Uptake pathway	Intracellular localization	Method	Toxicity	Ref.
Semi-conductor	QDs	QD 565 and QD 655, neutral (polyethylene glycol (PEG)), cationic (PEG–amine), or anionic (carboxylic acid) coatings	Human epidermal keratinocytes (HEKs)	20 nM; 24 h, 48 h	NM	Cytoplasm, cytoplasmic vacuole, nucleus	MTT, confocal laser scanning microscopy, and TEM	Cytotoxicity was observed for QD 565 and QD 655 coated with carboxylic acids or PEG–amine in 48 hours, with little cytotoxicity observed for PEG-coated QDs. Only carboxylic acid-coated QDs significantly increased release of IL-1β, IL-6, and IL-8	196
Semi-conductor	QDs	Tat peptide-conjugated quantum dots (Tat-QDs), emission peak wavelength – 655 nm	HeLa cells	1 nM; 1–24 h	Macropinocytosis	Cytoplasmic organelles, asymmetric perinuclear region (outside the cell nucleus)	Spinning disk confocal microscopy	NM	112

pathways through which they enter cells, with sizes ranging from over 1000 nm to less than 10 nm: phagocytosis, macro-pinocytosis, clathrin-mediated endocytosis, caveolin-mediated endocytosis, clathrin/caveolin-independent endocytosis, and direct cell membrane penetration.[167] Each pathway possesses its own limited size range and dynamics. The size range for phagocytosis is between 500 nm and 10 μm.[168] By contrast, most ligand-modified NMs, which are less than 500 nm, enter cells through endocytosis. To penetrate the cell membrane directly, the size of the material should be less than the thickness of the membrane bilayers, which is 4 to 10 nm. However, particles less than 5 nm are rapidly removed from the cell by renal clearance.[169–171]

The perfect size for NMs to be used in bio-applications such as drug delivery or cancer therapy has been the subject of much recent discussion. Chithrani *et al.* found that NMs with diameters <100 nm have strong size-dependent intracellular uptakes.[172] NPs with diameters of 14, 50, and 74 nm exhibit size-dependent cell uptake numbers and uptake halflife. NMs with 50 nm diameters exhibit higher cell uptake rates and numbers than the others because of the difference in wrapping time.[83] Jiang *et al.* found that the interaction between antibody (Herceptin)–Au NPs and SK-BR-3 breast cancer cell receptors is also size-dependent, and that NPs ranging from 25 to 50 nm in diameter exhibit the most efficient uptake.[173] The most efficient size, 50 nm, has been approximated by an experiment involving hydroxyapatite NPs (45 nm), other Au NPs (50 nm), and polypyrrole NPs (60 nm).[174–177] The size of the NMs also strongly influences uptake properties during phagocytosis. The highest phagocytosis occurs when the diameter ranges from 2 μm to 3 μm.[178] In addition, size must be considered because of NMs' toxic properties. Pan *et al.* found that 1.4 nm Au NPs exhibit high toxicity, whereas 15 nm Au NPs exhibit non-toxicity at 100-fold concentrations of 1.4 nm experiments.[179] The dramatic difference of the strong toxicity of Au clusters is because of the cluster size that facilitates combination with DNA and their major groove dimension.[180] Park *et al.* demonstrated that Ag NPs with a diameter of 20 nm are more toxic than larger NPs (80 nm and 113 nm) and Ag ions.[174]

The size of nanostructured materials is crucial to cell physiology in numerous bio-applications. The appropriate size of NPs for therapeutic treatment ranges from 10 nm to 100 nm, with larger particles limiting the diffusion in extracellular spaces. Moreover, diameters of 50 nm are appropriate for cellular uptake, drug delivery, and therapy for the ideal optical and size properties.

5.2 Effects of shape

The NM shape is another significant factor affecting the interaction between materials and cells. Tang's group pointed out that mesoporous silica NPs (MSNs) with different aspect ratios have major effects on cellular functions, such as uptake rate, cytoskeleton formation, adhesion, migration, viability, and proliferation.[181–183] The longer NR of MSNs (NLR450, aspect ratio ~ 4) is more easily internalized by A347 human melanoma cells compared with shorter NR (NLR240, aspect ratio ~ 2) and spherical (NS100, aspect ratio ~ 1) MSNs. In addition, the

cytotoxicity of the MSNs decreases as the aspect ratio decreases. Gratton *et al.* obtained similar results using cylindrical PRINT particles with varying aspect ratios.[184] High aspect ratio (d = 150 nm, h = 450 nm, aspect ratio = 3) rod-like particles are internalized more efficiently by HeLa cells than 200 nm symmetric cylindrical particles. Muro *et al.* investigated the targeted accumulation of various sizes (100 nm to 10 μm) and shapes (spherical *versus* elliptical disk-like particles) in endothelial cells, and discovered that the elliptical disks, which are micro-scale, had better targeting efficiency than any other spherical NPs.[185] However, the scale of NP changes at around or lower than 100 nm may present different results than those observed in previous discussions. Chan's group demonstrated that transferrin-coated spherical Au NPs (14 and 50 nm in diameter) showed higher uptake rates than transferrin-coated, rod-like Au NPs (aspect ratio = 1.5 (20 nm × 30 nm), 3.5 (14 nm × 50 nm), and 6 (7 nm × 42 nm)) for HeLa cells, with uncoated Au NPs presenting the same result.[83,172] Cell uptake efficiency also decreases as the aspect ratio increases. Florez *et al.* showed that nonspherical polymeric NPs (191 nm × 84 nm, 279 nm × 70 nm, and 381 nm × 65 nm) exhibit lower uptake efficiency than their spherical counterpart for mesenchymal stem cells (MSC) and HeLa cells, and the uptake rate decreases as the aspect ratio increases.[186] Qiu *et al.* compared spheres (30 nm × 33 nm) and rod-like Au NPs with various aspect ratios (40 nm × 21 nm, 50 nm × 17 nm, and 55 nm × 14 nm), resulting in the higher-aspect-ratio rod-like NPs being more slowly internalized than the lower-aspect-ratio rod-like and spherical Au NPs in MCF-7 cells.[122]

In the previous discussion, the interaction between the shape and size is shown to have a powerful effect on the biophysical reaction of cells, and the volume of the particles also seems to determine cell uptake efficiency. Moreover, the shape of NMs has also been proven by theoretical models and experimental studies to affect the internalization and vascular dynamics.[187–190] Nanostructured materials with controllable sizes and shapes, as well as their application have also been demonstrated.[191]

5.3 Effects of surface chemistry

The surface chemistry of NPs exerts various significant effects on cellular processes. The surface functional groups of NPs determine most of the physicochemical properties strongly related to further interaction between materials and cells. Among these physicochemical properties, the surface charge of NPs has the greatest effect on the interaction of NPs with cells. Cho *et al.* demonstrated that poly(vinyl alcohol) (PVA)-coated and citrate-coated Au NPs, which possess neutral and negative charges, respectively, absorb much less amounts on the negatively charged cell membranes than positively charged poly(allyamine hydrochloride) (PAA)-coated Au NPs, based on the I_2/KI etchant method. This method can selectively detect particles adhering to the cell surface.[192] The cellular uptake of positively charged NMs has resulted in higher uptake rates and efficiency in various cell types, as well as increased anionic particle adhesion to cell surfaces. These NMs include metal oxides,[193,194] metals,[195] QDs,[196] polymeric NPs,[197] mesoporous silica NPs,[198] *etc.* This faster cellular uptake and higher uptake efficiency can improve cellular entry in several bio-applications, including drug delivery systems or therapeutic behaviors.

Whether NPs are hydrophilic or hydrophobic is mostly determined by their surface ligands, surfactants, or stabilizers, which can be modified by chemical syntheses.[199] Hydrophobic NPs result in decreased dispersion in biological fluids and media.[200] However, the hydrophobic property enhances the penetration ability of NPs into cell membranes and nuclear pores through hydrophobic interaction.[201,202] As a result of attempts to balance dispersion property (hydrophilic) with high penetration ability (hydrophobic), amphiphilic NMs are attracting increased attention because of their excellent dispersion in both aqueous and organic phases.[203–206]

Surface modification is another topic for improving the bioavailability and decreasing the cytotoxicity of NMs.[200,207] Our previous work found that Au NRs synthesized with CTAB surface coating exhibit significant cytotoxicity to breast cancer MCF-7 cells, while further surface modification with PSS and PDDAC significantly decreased the toxicity of Au NRs and improved their cellular internalization.[122]

5.4 Effects of protein corona

To study the bio-interactions between NMs and cells, NMs are always introduced into the physiological environment, in which a large amount of amino acids, peptides and proteins are contained. When a NM enters a biological fluid, it rapidly adsorbs proteins and forms a protein corona.[208] The protein corona alters the size and surface composition of NMs, which further determine the physiological responses, including kinetics, transport, accumulation, exclusion and toxicity of NMs. The structure and composition of the protein corona depends on the characterization of the NMs, like size, shape and composition, the nature of the physiological environment like blood, interstitial fluid, cell cytoplasm and the duration of exposure.[209]

Protein corona has been observed with versatile NMs, such as Au NRs,[86,122] Au NPs,[210] SiO_2,[211] CNTs,[200] *etc.* For safe biomedical applications, it is critical that the interactions between NMs and cells are understood and controlled. Studies regarding the underlying mechanism of the dynamic protein adsorption process have been performed. Interactions between single-wall carbon nanotubes (SWCNTs) and human serum proteins were found to be a competitive mode of binding of these proteins with different adsorption capacities and packing modes.[200] The π–π stacking interactions between SWCNTs and aromatic residues (Trp, Phe, Tyr) are found to play a critical role in determining their adsorption capacity. Additional cellular cytotoxicity assays revealed that the competitive binding of blood proteins on the SWCNT surface can greatly alter their cellular interaction pathways and result in much reduced cytotoxicity for these protein-coated SWCNTs. In addition, the protein corona will affect the cellular internalization of NMs. Uptake of a NP–protein complex by cells depends on whether the cell membrane has receptors for the proteins, whether the proteins are presented in the correct orientation to interact with

the receptor, and whether the NP-bound protein can compete effectively with the free protein for the receptor.[212] A critical factor for controlling serum albumin binding is surface hydrophobicity, which in turn decreases the cellular uptake of NPs. Hydrophobic NPs bind albumin more tightly, inhibiting particle uptake, with a direct correlation observed between uptake and surface hydrophobicity.[213]

Despite substantial progress, detailed relationships between NMs and protein are still not clear. It is also unclear whether every protein in the corona influences the physiological response, or only a subset. Without this knowledge as a guide, it is difficult to design NMs to interact with proteins and cells in a controlled way.[214]

6 Summary and perspective

NMs have been investigated for several decades, and have also been applied to biological systems over the past decade. Chemical or physical synthesis can be used to alter such physical properties of NMs as morphology, size, and optical, electronic, or mechanical properties, for use in different applications. In biological systems, NMs can serve as media for the delivery of drugs, genes, or proteins for therapeutic treatments. The size of NPs enables them to enter cells by direct cell penetration or endocytosis. Moreover, the surfaces of nanostructured materials can be easily functionalized by chemical synthesis, and can be designed for more accurate treatments. Given the wide range of applications for NMs in living creatures, the interaction between NMs and cells has become a more significant research topic.

In this review, we summarize the NMs most commonly used in biomedical applications in the past decade. Owing to the different compositions, physical properties, and surface properties of these NMs, their use in the treatment of cells has resulted in various phenomena. Cellular uptake behaviors are strongly dependent on the size, shape, surface charge, and chemistry. The cytotoxicity of the materials is also related to several factors, including material composition, size, and surface ligands. The physicochemical properties of NMs should be traced from their synthesis procedures, intrinsic properties, and surface chemistry. Each material offers unique properties for use in different applications, but also has its specific limitations. We hope that this review will help the reader understand the basic interaction of cells and NMs.

Although numerous studies have examined the interaction between NPs and cells, much remains to be investigated. First, there are variable factors to be studied, such as the physical or chemical properties of materials, different cell lines, and the systematic study of specific materials. Second, shape conditions of NPs have not been well investigated. Third, the variations in the cell line result in different cell uptake, toxicity, or transportation in the same materials, but systematic studies of this phenomenon are scant. Fourth, the nanotoxicity issue and the accumulation of non-degradable materials relating to biosafety are yet to be understood. Fifth, the transformation of NMs' surface chemistry in living creatures is too complicated to investigate. Understanding the interactions between NMs and cells will improve the efficiency of these interactions. With the rapid increase in studies related to nanotechnology, investigation on NMs can be more beneficial than others because of their size. We believe that an extensive understanding of NM–bio interactions can serve as a foundation for future biomedical applications.

Acknowledgements

The authors thank the National Science Council (contract no. NSC 101-2113-M-002-014-MY3 and NSC 101-3113-P-002-021) for financially supporting this research. This work was also partly supported by the National Basic Research Program (2011CB933401) and the National Natural Science Foundation (31070854).

Notes and references

1 L. Dykman and N. Khlebtsov, *Chem. Soc. Rev.*, 2012, **41**, 2256–2282.
2 F. J. Ibanez and F. P. Zamborini, *Small*, 2012, **8**, 174–202.
3 M. B. Cortie and A. M. McDonagh, *Chem. Rev.*, 2011, **111**, 3713–3735.
4 A. Llevot and D. Astruc, *Chem. Soc. Rev.*, 2012, **41**, 242–257.
5 E. C. Dreaden, A. M. Alkilany, X. Huang, C. J. Murphy and M. A. El-Sayed, *Chem. Soc. Rev.*, 2012, **41**, 2740–2779.
6 S. Rana, A. Bajaj, R. Mout and V. M. Rotello, *Adv. Drug Delivery Rev.*, 2012, **64**, 200–216.
7 G. Y. Jing, H. L. Duan, X. M. Sun, Z. S. Zhang, J. Xu, Y. D. Li, J. X. Wang and D. P. Yu, *Phys. Rev. B: Condens. Matter Mater. Phys.*, 2006, **73**, 235409.
8 W. H. Ni, T. Ambjornsson, S. P. Apell, H. J. Chen and J. F. Wang, *Nano Lett.*, 2010, **10**, 77–84.
9 K. L. Kelly, E. Coronado, L. L. Zhao and G. C. Schatz, *J. Phys. Chem. B*, 2003, **107**, 668–677.
10 G. Schmid and B. Corain, *Eur. J. Inorg. Chem.*, 2003, 3081–3098.
11 P. Dutta, S. Pai, M. S. Seehra, N. Shah and G. P. Huffman, *J. Appl. Phys.*, 2009, **105**, 073104.
12 W. R. Algar, K. Susumu, J. B. Delehanty and I. L. Medintz, *Anal. Chem.*, 2011, **83**, 8826–8837.
13 S. Schafer, S. A. Wyrzgol, R. Caterino, A. Jentys, S. J. Schoell, M. Havecker, A. Knop-Gericke, J. A. Lercher, I. D. Sharp and M. Stutzmann, *J. Am. Chem. Soc.*, 2012, **134**, 12528–12535.
14 J. Turkevich, P. C. Stevenson and J. Hillier, *Discuss. Faraday Soc.*, 1951, **11**, 55–75.
15 P. C. Lee and D. Meisel, *J. Phys. Chem.*, 1982, **86**, 3391–3395.
16 M. C. Daniel and D. Astruc, *Chem. Rev.*, 2004, **104**, 293–346.
17 Y. G. Sun and Y. N. Xia, *Science*, 2002, **298**, 2176–2179.
18 N. R. Jana, L. Gearheart and C. J. Murphy, *Adv. Mater.*, 2001, **13**, 1389–1393.
19 H. M. Chen and R. S. Liu, *J. Phys. Chem. C*, 2011, **115**, 3513–3527.
20 L. C. Cheng, J. H. Huang, H. M. Chen, T. C. Lai, K. Y. Yang, R. S. Liu, M. Hsiao, C. H. Chen, L. J. Her and D. P. Tsai, *J. Mater. Chem.*, 2012, **22**, 2244–2253.

21 T. Ming, W. Feng, Q. Tang, F. Wang, L. D. Sun, J. F. Wang and C. H. Yan, *J. Am. Chem. Soc.*, 2009, **131**, 16350–16351.
22 S. S. Shankar, A. Rai, B. Ankamwar, A. Singh, A. Ahmad and M. Sastry, *Nat. Mater.*, 2004, **3**, 482–488.
23 M. L. Personick, M. R. Langille, J. Zhang, N. Harris, G. C. Schatz and C. A. Mirkin, *J. Am. Chem. Soc.*, 2011, **133**, 6170–6173.
24 H. Masuda, H. Tanaka and N. Baba, *Chem. Lett.*, 1990, 621–622.
25 Y. Y. Yu, S. S. Chang, C. L. Lee and C. R. C. Wang, *J. Phys. Chem. B*, 1997, **101**, 6661–6664.
26 N. R. Jana, L. Gearheart and C. J. Murphy, *J. Phys. Chem. B*, 2001, **105**, 4065–4067.
27 W. X. Niu, S. L. Zheng, D. W. Wang, X. Q. Liu, H. J. Li, S. A. Han, J. Chen, Z. Y. Tang and G. B. Xu, *J. Am. Chem. Soc.*, 2009, **131**, 697–703.
28 Y. Y. Ma, Q. Kuang, Z. Y. Jiang, Z. X. Xie, R. B. Huang and L. S. Zheng, *Angew. Chem., Int. Ed.*, 2008, **47**, 8901–8904.
29 Z. L. Wang, M. B. Mohamed, S. Link and M. A. El-Sayed, *Surf. Sci.*, 1999, **440**, L809–L814.
30 B. P. Khanal and E. R. Zubarev, *J. Am. Chem. Soc.*, 2008, **130**, 12634–12635.
31 E. Carbo-Argibay, B. Rodriguez-Gonzalez, J. Pacifico, I. Pastoriza-Santos, J. Perez-Juste and L. M. Liz-Marzan, *Angew. Chem., Int. Ed.*, 2007, **46**, 8983–8987.
32 S. E. Skrabalak, J. Y. Chen, Y. G. Sun, X. M. Lu, L. Au, C. M. Cobley and Y. N. Xia, *Acc. Chem. Res.*, 2008, **41**, 1587–1595.
33 T. Enoki, K. Takai, V. Osipov, M. Baidakova and A. Vul, *Chem.–Asian J.*, 2009, **4**, 796–804.
34 O. A. Shenderova, V. V. Zhirnov and D. W. Brenner, *Crit. Rev. Solid State Mater. Sci.*, 2002, **27**, 227–356.
35 A. Sinitskii and J. M. Tour, *IEEE Spectrum*, 2010, **47**, 28–33.
36 H. W. Kroto, J. R. Heath, S. C. Obrien, R. F. Curl and R. E. Smalley, *Nature*, 1985, **318**, 162–163.
37 A. F. Hebard, *Annu. Rev. Mater. Sci.*, 1993, **23**, 159–191.
38 B. Narymbetov, A. Omerzu, V. V. Kabanov, M. Tokumoto, H. Kobayashi and D. Mihailovic, *Nature*, 2000, **407**, 883–885.
39 L. Echegoyen and L. E. Echegoyen, *Acc. Chem. Res.*, 1998, **31**, 593–601.
40 D. M. Guldi and M. Prato, *Acc. Chem. Res.*, 2000, **33**, 695–703.
41 K. Miyazawa, *J. Nanosci. Nanotechnol.*, 2009, **9**, 41–50.
42 H. B. Liu, Y. L. Li, L. Jiang, H. Y. Luo, S. Q. Xiao, H. J. Fang, H. M. Li, D. B. Zhu, D. P. Yu, J. Xu and B. Xiang, *J. Am. Chem. Soc.*, 2002, **124**, 13370–13371.
43 L. Wang, B. B. Liu, S. D. Yu, M. G. Yao, D. D. Liu, Y. Y. Hou, T. Cui, G. T. Zou, B. Sundqvist, H. You, D. K. Zhang and D. G. Ma, *Chem. Mater.*, 2006, **18**, 4190–4194.
44 K. Miyazawa, K. Hamamoto, S. Nagata and T. Suga, *J. Mater. Res.*, 2003, **18**, 1096–1103.
45 M. Sathish, K. Miyazawa and T. Sasaki, *Chem. Mater.*, 2007, **19**, 2398–2400.
46 M. Sathish and K. Miyazawa, *J. Am. Chem. Soc.*, 2007, **129**, 13816–13817.
47 S. I. Cha, K. Miyazawa and J. D. Kim, *Chem. Mater.*, 2008, **20**, 1667–1669.
48 A. Masuhara, Z. Q. Tan, H. Kasai, H. Nakanishi and H. Oikawa, *Jpn. J. Appl. Phys.*, 2009, **48**, 050206.
49 A. Oberlin, M. Endo and T. Koyama, *J. Cryst. Growth*, 1976, **32**, 335–349.
50 S. Iijima, *Nature*, 1991, **354**, 56–58.
51 M. Endo, Y. A. Kim, T. Hayashi, K. Nishimura, T. Matusita, K. Miyashita and M. S. Dresselhaus, *Carbon*, 2001, **39**, 1287–1297.
52 N. Saito, Y. Usui, K. Aoki, N. Narita, M. Shimizu, K. Hara, N. Ogiwara, K. Nakamura, N. Ishigaki, H. Kato, S. Taruta and M. Endo, *Chem. Soc. Rev.*, 2009, **38**, 1897–1903.
53 Y. Saito, Y. Tani and A. Kasuya, *J. Phys. Chem. B*, 2000, **104**, 2495–2499.
54 E. Anglaret, S. Rols and J. L. Sauvajol, *Phys. Rev. Lett.*, 1998, **81**, 4780.
55 P. Vichchulada, M. A. Cauble, E. A. Abdi, E. I. Obi, Q. H. Zhang and M. D. Lay, *J. Phys. Chem. C*, 2010, **114**, 12490–12495.
56 S. A. Hodge, M. K. Bayazit, K. S. Coleman and M. S. P. Shaffer, *Chem. Soc. Rev.*, 2012, **41**, 4409–4429.
57 X. Z. Zhou, F. Boey and H. Zhang, *Chem. Soc. Rev.*, 2011, **40**, 5221–5231.
58 K. S. Novoselov, A. K. Geim, S. V. Morozov, D. Jiang, Y. Zhang, S. V. Dubonos, I. V. Grigorieva and A. A. Firsov, *Science*, 2004, **306**, 666–669.
59 D. V. Kosynkin, A. L. Higginbotham, A. Sinitskii, J. R. Lomeda, A. Dimiev, B. K. Price and J. M. Tour, *Nature*, 2009, **458**, 872–875.
60 A. Morelos-Gomez, S. M. Vega-Diaz, V. J. Gonzalez, F. Tristan-Lopez, R. Cruz-Silva, K. Fujisawa, H. Muramatsu, T. Hayashi, X. Mi, Y. F. Shi, H. Sakamoto, F. Khoerunnisa, K. Kaneko, B. G. Sumpter, Y. A. Kim, V. Meunier, M. Endo, E. Munoz-Sandoval and M. Terrones, *ACS Nano*, 2012, **6**, 2261–2272.
61 Y. M. A. Wu, Y. Fan, S. Speller, G. L. Creeth, J. T. Sadowski, K. He, A. W. Robertson, C. S. Allen and J. H. Warner, *ACS Nano*, 2012, **6**, 5010–5017.
62 C. Mattevi, H. Kim and M. Chhowalla, *J. Mater. Chem.*, 2011, **21**, 3324–3334.
63 S. Stankovich, D. A. Dikin, R. D. Piner, K. A. Kohlhaas, A. Kleinhammes, Y. Jia, Y. Wu, S. T. Nguyen and R. S. Ruoff, *Carbon*, 2007, **45**, 1558–1565.
64 S. Mayavan, J. B. Sim and S. M. Choi, *J. Mater. Chem.*, 2012, **22**, 6953–6958.
65 M. Pumera, *Energy Environ. Sci.*, 2011, **4**, 668–674.
66 M. Freitag, *Nat. Nanotechnol.*, 2008, **3**, 455–457.
67 R. M. Westervelt, *Science*, 2008, **320**, 324–325.
68 R. S. Sundaram, M. Steiner, H. Y. Chiu, M. Engel, A. A. Bol, R. Krupke, M. Burghard, K. Kern and P. Avouris, *Nano Lett.*, 2011, **11**, 3833–3837.
69 H. Shen, L. M. Zhang, M. Liu and Z. J. Zhang, *Theranostics*, 2012, **2**, 283–294.
70 A. P. Alivisatos, *J. Phys. Chem.*, 1996, **100**, 13226–13239.
71 P. Zrazhevskiy, M. Sena and X. Gao, *Chem. Soc. Rev.*, 2010, **39**, 4326–4354.

72 C. B. Murray, D. J. Norris and M. G. Bawendi, *J. Am. Chem. Soc.*, 1993, **115**, 8706–8715.
73 Z. A. Peng and X. G. Peng, *J. Am. Chem. Soc.*, 2001, **123**, 183–184.
74 L. H. Qu, Z. A. Peng and X. G. Peng, *Nano Lett.*, 2001, **1**, 333–337.
75 Z. A. Peng and X. G. Peng, *J. Am. Chem. Soc.*, 2002, **124**, 3343–3353.
76 V. Biju, T. Itoh and M. Ishikawa, *Chem. Soc. Rev.*, 2010, **39**, 3031–3056.
77 X. G. Peng, L. Manna, W. D. Yang, J. Wickham, E. Scher, A. Kadavanich and A. P. Alivisatos, *Nature*, 2000, **404**, 59–61.
78 D. V. Talapin, J. H. Nelson, E. V. Shevchenko, S. Aloni, B. Sadtler and A. P. Alivisatos, *Nano Lett.*, 2007, **7**, 2951–2959.
79 F. Zhao, Y. Zhao, Y. Liu, X. Chang and C. Chen, *Small*, 2011, **7**, 1322–1337.
80 B. D. Chithrani, J. Stewart, C. Allen and D. A. Jaffray, *Nanomedicine*, 2009, **5**, 118–127.
81 D. B. Peckys and N. de Jonge, *Nano Lett.*, 2011, **11**, 1733–1738.
82 A. Albanese and W. C. W. Chan, *ACS Nano*, 2011, **5**, 5478–5489.
83 B. D. Chithrani and W. C. W. Chan, *Nano Lett.*, 2007, **7**, 1542–1550.
84 Q. Zhang, V. M. Hitchins, A. M. Schrand, S. M. Hussain and P. L. Goering, *Nanotoxicology*, 2011, **5**, 284–295.
85 Y. J. Gu, J. Cheng, C. C. Lin, Y. W. Lam, S. H. Cheng and W. T. Wong, *Toxicol. Appl. Pharmacol.*, 2009, **237**, 196–204.
86 L. Wang, Y. Liu, W. Li, X. Jiang, Y. Ji, X. Wu, L. Xu, Y. Qiu, K. Zhao, T. Wei, Y. Li, Y. Zhao and C. Chen, *Nano Lett.*, 2010, **11**, 772–780.
87 P. Nativo, I. A. Prior and M. Brust, *ACS Nano*, 2008, **2**, 1639–1644.
88 A. K. Oyelere, P. C. Chen, X. Huang, I. H. El-Sayed and M. A. El-Sayed, *Bioconjugate Chem.*, 2007, **18**, 1490–1497.
89 S. W. P. Wijnhoven, W. J. G. M. Peijnenburg, C. A. Herberts, W. I. Hagens, A. G. Oomen, E. H. W. Heugens, B. Roszek, J. Bisschops, I. Gosens and D. Van De Meent, *Nanotoxicology*, 2009, **3**, 109–138.
90 S. Hackenberg, A. Scherzed, M. Kessler, S. Hummel, A. Technau, K. Froelich, C. Ginzkey, C. Koehler, R. Hagen and N. Kleinsasser, *Toxicol. Lett.*, 2011, **201**, 27–33.
91 P. AshaRani, G. Low Kah Mun, M. P. Hande and S. Valiyaveettil, *ACS Nano*, 2008, **3**, 279–290.
92 H. R. Kim, M. J. Kim, S. Y. Lee, S. M. Oh and K. H. Chung, *Mutat. Res.*, 2011, **726**, 129–135.
93 L. Wei, J. Tang, Z. Zhang, Y. Chen, G. Zhou and T. Xi, *Biomed. Mater.*, 2010, **5**, 044103.
94 M. Ahamed, M. Karns, M. Goodson, J. Rowe, S. M. Hussain, J. J. Schlager and Y. Hong, *Toxicol. Appl. Pharmacol.*, 2008, **233**, 404–410.
95 A. E. Porter, K. Muller, J. Skepper, P. Midgley and M. Welland, *Acta Biomater.*, 2006, **2**, 409–419.
96 M. Raoof, Y. Mackeyev, M. A. Cheney, L. J. Wilson and S. A. Curley, *Biomaterials*, 2012, **33**, 2952–2960.
97 F. Lao, L. Chen, W. Li, C. Ge, Y. Qu, Q. Sun, Y. Zhao, D. Han and C. Chen, *ACS Nano*, 2009, **3**, 3358–3368.
98 W. Li, C. Chen, C. Ye, T. Wei, Y. Zhao, F. Lao, Z. Chen, H. Meng, Y. Gao and H. Yuan, *Nanotechnology*, 2008, **19**, 145102.
99 A. Dellinger, Z. Zhou, S. K. Norton, R. Lenk, D. Conrad and C. L. Kepley, *Nanomedicine*, 2010, **6**, 575–582.
100 Y. Liu, Y. Zhao, B. Sun and C. Chen, *Acc. Chem. Res.*, 2013, **46**, 702–713.
101 L. Lacerda, G. Pastorin, D. Gathercole, J. Buddle, M. Prato, A. Bianco and K. Kostarelos, *Adv. Mater.*, 2007, **19**, 1480–1484.
102 B. Kang, D. Yu, S. Chang, D. Chen, Y. Dai and Y. Ding, *Nanotechnology*, 2008, **19**, 375103.
103 A. E. Porter, M. Gass, J. S. Bendall, K. Muller, A. Goode, J. N. Skepper, P. A. Midgley and M. Welland, *ACS Nano*, 2009, **3**, 1485–1492.
104 D. Pantarotto, J. P. Briand, M. Prato and A. Bianco, *Chem. Commun.*, 2004, 16–17.
105 E. Mooney, P. Dockery, U. Greiser, M. Murphy and V. Barron, *Nano Lett.*, 2008, **8**, 2137–2143.
106 J. Cheng, K. A. S. Fernando, L. M. Veca, Y. P. Sun, A. I. Lamond, Y. W. Lam and S. H. Cheng, *ACS Nano*, 2008, **2**, 2085–2094.
107 H. Jin, D. A. Heller and M. S. Strano, *Nano Lett.*, 2008, **8**, 1577–1585.
108 Q. Mu, D. L. Broughton and B. Yan, *Nano Lett.*, 2009, **9**, 4370–4375.
109 G. Y. Chen, D. W. P. Pang, S. M. Hwang, H. Y. Tuan and Y. C. Hu, *Biomaterials*, 2012, **33**, 418–427.
110 H. Yue, W. Wei, Z. G. Yue, B. Wang, N. N. Luo, Y. J. Gao, D. Ma, G. H. Ma and Z. G. Su, *Biomaterials*, 2012, **33**, 4013–4021.
111 L. W. Zhang and N. A. Monteiro-Riviere, *Toxicol. Sci.*, 2009, **110**, 138–155.
112 G. Ruan, A. Agrawal, A. I. Marcus and S. Nie, *J. Am. Chem. Soc.*, 2007, **129**, 14759–14766.
113 J. Lovrić, H. S. Bazzi, Y. Cuie, G. R. A. Fortin, F. M. Winnik and D. Maysinger, *J. Mol. Med.*, 2005, **83**, 377–385.
114 L. W. Zhang, W. Bäumer and N. A. Monteiro-Riviere, *Nanomedicine*, 2011, **6**, 777–791.
115 Y. Zhang, M. K. So and J. Rao, *Nano Lett.*, 2006, **6**, 1988–1992.
116 J. K. Jaiswal, H. Mattoussi, J. M. Mauro and S. M. Simon, *Nat. Biotechnol.*, 2002, **21**, 47–51.
117 H. Duan and S. Nie, *J. Am. Chem. Soc.*, 2007, **129**, 3333–3338.
118 S. Wang, W. Lu, O. Tovmachenko, U. S. Rai, H. Yu and P. C. Ray, *Chem. Phys. Lett.*, 2008, **463**, 145–149.
119 A. M. Alkilany, P. K. Nagaria, C. R. Hexel, T. J. Shaw, C. J. Murphy and M. D. Wyatt, *Small*, 2009, **5**, 701–708.
120 H. J. Parab, H. M. Chen, T.-C. Lai, J. H. Huang, P. H. Chen, R.-S. Liu, M. Hsiao, C.-H. Chen, D.-P. Tsai and Y.-K. Hwu, *J. Phys. Chem. C*, 2009, **113**, 7574–7578.
121 T. S. Hauck, A. A. Ghazani and W. C. W. Chan, *Small*, 2007, **4**, 153–159.
122 Y. Qiu, Y. Liu, L. Wang, L. Xu, R. Bai, Y. Ji, X. Wu, Y. Zhao, Y. Li and C. Chen, *Biomaterials*, 2010, **31**, 7606–7619.

123 Y. J. Kim, S. I. Yang and J. C. Ryu, *Mol. Cell. Toxicol.*, 2010, **6**, 119–125.
124 R. Foldbjerg, D. A. Dang and H. Autrup, *Arch. Toxicol.*, 2011, **85**, 743–750.
125 S. Arora, J. Jain, J. Rajwade and K. Paknikar, *Toxicol. Lett.*, 2008, **179**, 93–100.
126 C. Carlson, S. Hussain, A. Schrand, L. K. Braydich-Stolle, K. Hess, R. Jones and J. Schlager, *J. Phys. Chem. B*, 2008, **112**, 13608–13619.
127 S. Kim, J. E. Choi, J. Choi, K. H. Chung, K. Park, J. Yi and D. Y. Ryu, *Toxicol. In Vitro*, 2009, **23**, 1076–1084.
128 R. Foldbjerg, P. Olesen, M. Hougaard, D. A. Dang, H. J. Hoffmann and H. Autrup, *Toxicol. Lett.*, 2009, **190**, 156–162.
129 S. Liau, D. Read, W. Pugh, J. Furr and A. Russell, *Lett. Appl. Microbiol.*, 1997, **25**, 279–283.
130 E. Navarro, F. Piccapietra, B. Wagner, F. Marconi, R. Kaegi, N. Odzak, L. Sigg and R. Behra, *Environ. Sci. Technol.*, 2008, **42**, 8959–8964.
131 C. Beer, R. Foldbjerg, Y. Hayashi and H. Autrup, *Toxicol. Lett.*, 2012, **208**, 286–292.
132 E. Oberdörster, *Environ. Health Perspect.*, 2004, **112**, 1058–1062.
133 Y. Niwa and N. Iwai, *Environ. Health Prev. Med.*, 2006, **11**, 292–297.
134 C. M. Sayes, A. M. Gobin, K. D. Ausman, J. Mendez, J. L. West and V. L. Colvin, *Biomaterials*, 2005, **26**, 7587–7595.
135 C. M. Sayes, J. D. Fortner, W. Guo, D. Lyon, A. M. Boyd, K. D. Ausman, Y. J. Tao, B. Sitharaman, L. J. Wilson and J. B. Hughes, *Nano Lett.*, 2004, **4**, 1881–1887.
136 A. Don Porto Carero, P. Hoet, L. Verschaeve, G. Schoeters and B. Nemery, *Environ. Mol. Mutagen.*, 2001, **37**, 155–163.
137 L. Braydich-Stolle, S. Hussain, J. J. Schlager and M. C. Hofmann, *Toxicol. Sci.*, 2005, **88**, 412–419.
138 Y. Zhang, S. F. Ali, E. Dervishi, Y. Xu, Z. Li, D. Casciano and A. S. Biris, *ACS Nano*, 2010, **4**, 3181–3186.
139 S. Hirano, Y. Fujitani, A. Furuyama and S. Kanno, *Toxicol. Appl. Pharmacol.*, 2010, **249**, 8–15.
140 B. Zhong, W. Whong and T. Ong, *Mutat. Res., Genet. Toxicol. Environ. Mutagen.*, 1997, **393**, 181–187.
141 C. Ge, F. Lao, W. Li, Y. Li, C. Chen, Y. Qiu, X. Mao, B. Li, Z. Chai and Y. Zhao, *Anal. Chem.*, 2008, **80**, 9426–9634.
142 N. W. S. Kam, T. C. Jessop, P. A. Wender and H. Dai, *J. Am. Chem. Soc.*, 2004, **126**, 6850–6851.
143 L. W. Zhang, L. Zeng, A. R. Barron and N. A. Monteiro-Riviere, *Internet J. Toxicol.*, 2007, **26**, 103–113.
144 A. A. Shvedova, A. Pietroiusti, B. Fadeel and V. E. Kagan, *Toxicol. Appl. Pharmacol.*, 2012, **261**, 121–133.
145 C. C. Ge, Y. Li, J. J. Yin, Y. Liu, L. M. Wang, Y. L. Zhao and C. Y. Chen, *NPG Asia Mater.*, 2012, **4**, e32.
146 L. Meng, R. Chen, L. M. Wang, P. Wang, C. Z. Li, R. Bai, Y. L. Zhao, H. Autrup and C. Y. Chen, *Small*, DOI: 10.1002/smll.201201388, ASAP.
147 I. Fenoglio, M. Tomatis, D. Lison, J. Muller, A. Fonseca, J. B. Nagy and B. Fubini, *Free Radical Biol. Med.*, 2006, **40**, 1227–1233.
148 L. Meng, A. Jiang, R. Chen, C. Li, L. Wang, Y. Qu, P. Wang, Y. Zhao and C. Chen, *Toxicology*, 2012, DOI: 10.1016/j.tox.2012.11.011, ASAP.
149 V. Raffa, G. Ciofani, O. Vittorio, C. Riggio and A. Cuschieri, *Nanomedicine*, 2010, **5**, 89–97.
150 L. Lacerda, H. Ali-Boucetta, M. A. Herrero, G. Pastorin, A. Bianco, M. Prato and K. Kostarelos, *Nanomedicine*, 2008, **3**, 149–161.
151 X. Sun, Z. Liu, K. Welsher, J. T. Robinson, A. Goodwin, S. Zaric and H. Dai, *Nano Res.*, 2008, **1**, 203–212.
152 K. Yang, S. Zhang, G. Zhang, X. Sun, S. T. Lee and Z. Liu, *Nano Lett.*, 2010, **10**, 3318–3323.
153 W. Hu, C. Peng, W. Luo, M. Lv, X. Li, D. Li, Q. Huang and C. Fan, *ACS Nano*, 2010, **4**, 4317–4323.
154 K. Wang, J. Ruan, H. Song, J. Zhang, Y. Wo, S. Guo and D. Cui, *Nanoscale Res. Lett.*, 2011, **6**, 8.
155 S. R. Ryoo, Y. K. Kim, M. H. Kim and D. H. Min, *ACS Nano*, 2010, **4**, 6587–6598.
156 Y. Chang, S. T. Yang, J. H. Liu, E. Dong, Y. Wang, A. Cao, Y. Liu and H. Wang, *Toxicol. Lett.*, 2011, **200**, 201–210.
157 P. Rivera Gil, G. Oberdörster, A. Elder, V. Puntes and W. J. Parak, *ACS Nano*, 2010, **4**, 5527–5531.
158 A. Sasidharan, L. Panchakarla, P. Chandran, D. Menon, S. Nair, C. Rao and M. Koyakutty, *Nanoscale*, 2011, **3**, 2461–2464.
159 Y. Li, Y. Liu, Y. Fu, T. Wei, L. Le Guyader, G. Gao, R. S. Liu, Y. Z. Chang and C. Chen, *Biomaterials*, 2012, **33**, 402–411.
160 H. Zhou, K. Zhao, W. Li, N. Yang, Y. Liu, C. Chen and T. Wei, *Biomaterials*, 2012, **33**, 6933–6942.
161 E. Chang, N. Thekkek, W. W. Yu, V. L. Colvin and R. Drezek, *Small*, 2006, **2**, 1412–1417.
162 A. Hoshino, K. Fujioka, T. Oku, M. Suga, Y. F. Sasaki, T. Ohta, M. Yasuhara, K. Suzuki and K. Yamamoto, *Nano Lett.*, 2004, **4**, 2163–2169.
163 A. M. Derfus, W. C. W. Chan and S. N. Bhatia, *Nano Lett.*, 2004, **4**, 11–18.
164 M. A. Hines and P. Guyot-Sionnest, *J. Phys. Chem.*, 1996, **100**, 468–471.
165 X. Peng, M. C. Schlamp, A. V. Kadavanich and A. Alivisatos, *J. Am. Chem. Soc.*, 1997, **119**, 7019–7029.
166 N. A. Monteiro-Riviere and A. O. Inman, *Carbon*, 2006, **44**, 1070–1078.
167 M. Zhu, G. Nie, H. Meng, T. Xia, A. Nel and Y. Zhao, *Acc. Chem. Res.*, 2013, **46**, 622–631.
168 S. Mitragotri and J. Lahann, *Nat. Mater.*, 2009, **8**, 15–23.
169 H. S. Choi, W. Liu, P. Misra, E. Tanaka, J. P. Zimmer, B. I. Ipe, M. G. Bawendi and J. V. Frangioni, *Nat. Biotechnol.*, 2007, **25**, 1165–1170.
170 F. Lux, A. Mignot, P. Mowat, C. Louis, S. Dufort, C. Bernhard, F. Denat, F. Boschetti, C. Brunet, R. Antoine, P. Dugourd, S. Laurent, L. Vander Elst, R. Muller, L. Sancey, V. Josserand, J. L. Coll, V. Stupar, E. Barbier, C. Remy, A. Broisat, C. Ghezzi, G. Le Duc, S. Roux, P. Perriat and O. Tillement, *Angew. Chem., Int. Ed.*, 2011, **50**, 12299–12303.
171 C. Zhou, M. Long, Y. P. Qin, X. K. Sun and J. Zheng, *Angew. Chem., Int. Ed.*, 2011, **50**, 3168–3172.

172 B. D. Chithrani, A. A. Ghazani and W. C. W. Chan, *Nano Lett.*, 2006, **6**, 662–668.
173 W. Jiang, B. Y. S. Kim, J. T. Rutka and W. C. W. Chan, *Nat. Nanotechnol.*, 2008, **3**, 145–150.
174 M. V. D. Z. Park, A. M. Neigh, J. P. Vermeulen, L. J. J. de la Fonteyne, H. W. Verharen, J. J. Briede, H. van Loveren and W. H. de Jong, *Biomaterials*, 2011, **32**, 9810–9817.
175 Y. Yuan, C. S. Liu, J. C. Qjan, J. Wang and Y. Zhang, *Biomaterials*, 2010, **31**, 730–740.
176 X. W. Ma, Y. Y. Wu, S. B. Jin, Y. Tian, X. N. Zhang, Y. L. Zhao, L. Yu and X. J. Liang, *ACS Nano*, 2011, **5**, 8629–8639.
177 S. Kim, W. K. Oh, Y. S. Jeong, J. Y. Hong, B. R. Cho, J. S. Hahn and J. Jang, *Biomaterials*, 2011, **32**, 2342–2350.
178 J. A. Champion, A. Walker and S. Mitragotri, *Pharm. Res.*, 2008, **25**, 1815–1821.
179 Y. Pan, S. Neuss, A. Leifert, M. Fischler, F. Wen, U. Simon, G. Schmid, W. Brandau and W. Jahnen-Dechent, *Small*, 2007, **3**, 1941–1949.
180 M. Tsoli, H. Kuhn, W. Brandau, H. Esche and G. Schmid, *Small*, 2005, **1**, 841–844.
181 N. J. Hao, L. L. Li, Q. Zhang, X. L. Huang, X. W. Meng, Y. Q. Zhang, D. Chen, F. Q. Tang and L. F. Li, *Microporous Mesoporous Mater.*, 2012, **162**, 14–23.
182 X. L. Huang, L. L. Li, T. L. Liu, N. J. Hao, H. Y. Liu, D. Chen and F. Q. Tang, *ACS Nano*, 2011, **5**, 5390–5399.
183 X. L. Huang, X. Teng, D. Chen, F. Q. Tang and J. Q. He, *Biomaterials*, 2010, **31**, 438–448.
184 S. E. A. Gratton, P. A. Ropp, P. D. Pohlhaus, J. C. Luft, V. J. Madden, M. E. Napier and J. M. DeSimone, *Proc. Natl. Acad. Sci. U. S. A.*, 2008, **105**, 11613–11618.
185 S. Muro, C. Garnacho, J. A. Champion, J. Leferovich, C. Gajewski, E. H. Schuchman, S. Mitragotri and V. R. Muzykantov, *Mol. Ther.*, 2008, **16**, 1450–1458.
186 L. Florez, C. Herrmann, J. M. Cramer, C. P. Hauser, K. Koynov, K. Landfester, D. Crespy and V. Mailander, *Small*, 2012, **8**, 2222–2230.
187 J. A. Champion and S. Mitragotri, *Proc. Natl. Acad. Sci. U. S. A.*, 2006, **103**, 4930–4934.
188 P. Decuzzi, R. Pasqualini, W. Arap and M. Ferrari, *Pharm. Res.*, 2009, **26**, 235–243.
189 P. Decuzzi and M. Ferrari, *Biomaterials*, 2006, **27**, 5307–5314.
190 P. Decuzzi, B. Godin, T. Tanaka, S. Y. Lee, C. Chiappini, X. Liu and M. Ferrari, *J. Controlled Release*, 2010, **141**, 320–327.
191 R. S. Liu, *Controlled Nanofabrication: Advances and Applications*, Pan Stanford Publishing, Singapore, 2013.
192 E. C. Cho, J. W. Xie, P. A. Wurm and Y. N. Xia, *Nano Lett.*, 2009, **9**, 1080–1084.
193 C. Wilhelm, C. Billotey, J. Roger, J. N. Pons, J. C. Bacri and F. Gazeau, *Biomaterials*, 2003, **24**, 1001–1011.
194 A. L. Martin, L. M. Bernas, B. K. Rutt, P. J. Foster and E. R. Gillies, *Bioconjugate Chem.*, 2008, **19**, 2375–2384.
195 R. R. Arvizo, O. R. Miranda, M. A. Thompson, C. M. Pabelick, R. Bhattacharya, J. D. Robertson, V. M. Rotello, Y. S. Prakash and P. Mukherjee, *Nano Lett.*, 2010, **10**, 2543–2548.
196 J. P. Ryman-Rasmussen, J. E. Riviere and N. A. Monteiro-Riviere, *Nano Lett.*, 2007, **7**, 1344–1348.
197 O. Harush-Frenkel, N. Debotton, S. Benita and Y. Altschuler, *Biochem. Biophys. Res. Commun.*, 2007, **353**, 26–32.
198 T. Xia, M. Kovochich, M. Liong, H. Meng, S. Kabehie, S. George, J. I. Zink and A. E. Nel, *ACS Nano*, 2009, **3**, 3273–3286.
199 A. E. Nel, L. Madler, D. Velegol, T. Xia, E. M. V. Hoek, P. Somasundaran, F. Klaessig, V. Castranova and M. Thompson, *Nat. Mater.*, 2009, **8**, 543–557.
200 C. C. Ge, J. F. Du, L. N. Zhao, L. M. Wang, Y. Liu, D. H. Li, Y. L. Yang, R. H. Zhou, Y. L. Zhao, Z. F. Chai and C. Y. Chen, *Proc. Natl. Acad. Sci. U. S. A.*, 2011, **108**, 16968–16973.
201 S. J. Tan, N. R. Jana, S. J. Gao, P. K. Patra and J. Y. Ying, *Chem. Mater.*, 2010, **22**, 2239–2247.
202 B. Naim, D. Zbaida, S. Dagan, R. Kapon and Z. Reich, *EMBO J.*, 2009, **28**, 2697–2705.
203 E. R. Zubarev, J. Xu, A. Sayyad and J. D. Gibson, *J. Am. Chem. Soc.*, 2006, **128**, 15098–15099.
204 H. W. Duan, M. Kuang, D. Y. Wang, D. G. Kurth and H. Mohwald, *Angew. Chem., Int. Ed.*, 2005, **44**, 1717–1720.
205 H. Wang, Y. Zhao, Y. Wu, Y. L. Hu, K. H. Nan, G. J. Nie and H. Chen, *Biomaterials*, 2011, **32**, 8281–8290.
206 Q. Xu, Y. Liu, S. Su, W. Li, C. Chen and Y. Wu, *Biomaterials*, 2012, **33**, 1627–1639.
207 R. Gref, Y. Minamitake, M. T. Peracchia, V. Trubetskoy, V. Torchilin and R. Langer, *Science*, 1994, **263**, 1600–1603.
208 I. Lynch and K. A. Dawson, *Nano Today*, 2008, **3**, 40–47.
209 C. D. Walkey and W. C. W. Chan, *Chem. Soc. Rev.*, 2012, **41**, 2780–2799.
210 M. A. Dobrovolskaia, A. K. Patri, J. W. Zheng, J. D. Clogston, N. Ayub, P. Aggarwal, B. W. Neun, J. B. Hall and S. E. McNeil, *Nanomedicine*, 2009, **5**, 106–117.
211 M. P. Monopoli, D. Walczyk, A. Campbell, G. Elia, I. Lynch, F. B. Bombelli and K. A. Dawson, *J. Am. Chem. Soc.*, 2011, **133**, 2525–2534.
212 I. Lynch, A. Salvati and K. A. Dawson, *Nat. Nanotechnol.*, 2009, **4**, 546–547.
213 Z. J. Zhu, T. Posati, D. F. Moyano, R. Tang, B. Yan, R. W. Vachet and V. M. Rotello, *Small*, 2012, **8**, 2659–2663.
214 C. D. Walkey and W. C. W. Chan, *Chem. Soc. Rev.*, 2012, **41**, 2780–2799.
215 P. V. AshaRani, G. L. K. Mun, M. P. Hande and S. Valiyaveettil, *ACS Nano*, 2009, **3**, 279–290.
216 Y. Zhu, W. X. Li, Q. N. Li, Y. G. Li, Y. F. Li, X. Y. Zhang and Q. Huang, *Carbon*, 2009, **47**, 1351–1358.